Energy Reports 10 (2023) 3757–3779

Contents lists available at ScienceDirect

Energy Reports

journal homepage: www.elsevier.com/locate/egyr

Review article

Analysis of heat transfer in various cavity geometries with and without nano-enhanced phase change material: A review

Farhan Lafta Rashid [a], Hayder I. Mohammed [b], Anmar Dulaimi [c,d,*], Mudhar A. Al-Obaidi [e,f], Pouyan Talebizadehsardari [g], Shabbir Ahmad [h], Arman Ameen [i,**]

[a] Petroleum Engineering Department, College of Engineering, University of Kerbala, Karbala 56001, Iraq
[b] Department of Physics, College of Education, University of Garmian, Kalar 46021, Kurdistan, Iraq
[c] College of Engineering, University of Warith Al-Anbiyaa, Karbala 56001, Iraq
[d] School of Civil Engineering and Built Environment, Liverpool John Moores University, Liverpool L3 2ET, UK
[e] Technical Institute of Baquba, Middle Technical University, Baghdad 10074, Iraq
[f] Technical Instructor Training Institute, Middle Technical University, Baghdad 10074, Iraq
[g] Institute of Geophysics and Geomatics, China University of Geosciences, Wuhan 430074, China
[h] Department of Basic Sciences and Humanities, Muhammad Nawaz Sharif University of Engineering and Technology, Multan 60000, Pakistan
[i] Department of Building Engineering, Energy Systems and Sustainability Science, University of Gävle, 801 76 Gävle, Sweden

ARTICLE INFO

Keywords:
Heat transfer
Cavity
Review
Thermal energy storage

ABSTRACT

Numerous heating and cooling design methods, including energy storage, geothermal resources, heaters, solar collectors, underground water movement, lakes, and nuclear reactors, require the study of flow regimes in a cavity and their impact on thermal efficiency in heat transportation. Despite the existence of several review studies in the open literature, there is no specific review of heat transfer investigations that consider different cavity designs, such as spheres, squares, trapezoids, and triangles. Therefore, this work aims to conduct a comprehensive review of previous research published between 2016 and 2023 on heat transfer analysis in these cavity designs. The intention is to clarify how various cavity shapes perform in terms of flow and heat transfer, both with and without the addition of nano-enhanced phase change materials (NePCMs), which may include fins, obstacles, cylinders, and baffles. The study also explores the influence of factors like thermophoresis, buoyancy, magnetic forces, and others on heat transport in cavities. Additionally, it investigates the role of air, water, nanofluids, and hybrid nanofluids within cavities. According to the reviewed research, nanoparticles in the base fluid speed up the cooling process and reduce the required discharging time. Thermophoresis, where nanoparticles move from the heated wall to the cold nanofluid flow, becomes more pronounced with increasing Reynolds numbers. Increasing the heated area of the lower flat fin enhances the heat transfer rate, while increasing both the Rayleigh number and the solid volume percentage of nanoparticles reduces it. Radiation blockage alters the path of hot particles and affects the anticipated radiative amount. Optical thickness plays a role in rapidly cooling a medium, and partition thickness has the most significant effect on heat transport when the thermal conductivity ratio is low. Heat transmission is most improved when the Rayleigh number is high and the Richardson number is low.

Abbreviation: AR, Aspect ratio; Be, Bejan number (-); CFD, Computational fluid dynamics; FEM, Finite element method; GCI, Grid convergence index; GFEM, Galerkin finite element technique; Gr, Grashof number (-); Ha, Hartmann number (-); HTR, Heat transfer rate; Kn, Knudsen number (-); LBM, Lattice Boltzmann method; LHTES, Latent heat thermal energy storage; MCHS, Microchannel heat sinks; MHD, Magneto hydrodynamics; MHX, Microchannel heat exchanger; NePCM, Nano-enhanced phase change material; Nu, Nusselt number (-); ODE, Ordinary differential equation; PCM, Phase change materials; Pr, Prandtl Number (-); Ra, Rayleigh number (-); Rd, Radiation parameter; Ri, Richardson number (-); RSM, Response Surface Method; SWCNTs, Single Wall Carbon Nanotubes.

* Corresponding author at: College of Engineering, University of Warith Al-Anbiyaa, Karbala 56001, Iraq.
** Corresponding author.
E-mail addresses: a.f.dulaimi@ljmu.ac.uk (A. Dulaimi), arman.ameen@hig.se (A. Ameen).

https://doi.org/10.1016/j.egyr.2023.10.036
Received 25 July 2023; Received in revised form 12 September 2023; Accepted 9 October 2023
Available online 18 October 2023

1. Introduction

Latent heat thermal energy storage (LHTES) has long been researched concerning the thermal charging of phase change materials (PCMs) in the domain or over exterior bodies (Fukusako and Yamada, 1999; Rashid et al., 2023a, 2023b).

The remarkable preparation and chemical and mechanical stability of PCMs are well known. Precise phase transitions at desired temperature ranges are made possible by rigorous quality control throughout PCM manufacture, which also guarantees uniformity and purity. They are trustworthy for long-term applications because of their strong chemical stability, which guarantees less deterioration over several temperature cycles. Their mechanical durability guarantees that they can survive the strains of varied systems, ensuring constant and dependable performance in a variety of thermal energy storage (TES) and management applications (Qin et al., 2019).

PCMs have a variety of practical applications in engineering and industry. For instance, PCMs were used as TES systems because of their capacity to store and release energy during phase transitions. Also, PCMs are used in solar thermal systems to store the heat energy produced by sunshine during the day and release it at night or when it is cloudy (Rashid et al., 2023c). As a result, solar power systems are more effective and reliable. For thermal regulation in structures, PCM-enhanced building materials like concrete or plaster are used (Rashid et al., 2023d). By maintaining comfortable indoor temperatures, they can cut heating and cooling expenses. The containers of PCM often have the form of cubes, rectangles, squares, cylinders, spheres, and annular tubes (Dhaidan and Khodadadi, 2015). PCMs contained within a polymer shell are known as polymer-encapsulated phase change materials (PE-PCMs), which improve their thermal stability and allow for regulated heat release or absorption. These cutting-edge materials are used in thermal management systems and energy-efficient construction materials (Hong et al., 2010). In addition to being the favoured structure for encapsulation components in packed bed LHTES units with high storage density and high heat transfer performance (Regin et al., 2008), the spherical shape is also a representative geometry for posing a one-dimensional Stefan issue on convective heat charging/discharging, which has straightforward approximatively/numerical solutions (Regin et al., 2008).

Researchers have been trying to model the effect of different temperatures on spontaneous convection in an empty enclosure (Corcione, 2003; Ouertatani et al., 2008; Rashid et al., 2022a; Tiji et al., 2022) for decades. A primary enclosure with no interior body is more accessible than one with fluid flow and natural heat transfer from a hot body, particularly a cylinder within. For this reason, many studies (Ha et al., 2002; Lee et al., 2004; De and Dalal, 2006; Gangawane and Manikandan, 2017;) have examined how a hot inner body of varying geometries influences natural convection heat transport inside a square enclosure.

Incorporating nanoparticles into conventional PCMs to improve their thermal properties is the fundamental chemistry of nano-enhanced PCMs (NePCM). For their high thermal conductivity, nanoparticles made of substances like copper, carbon, or metal oxides are frequently used in this context. These nanoparticles are distributed throughout the PCM and have had their surfaces modified to stop them from aggregating. The nanoparticles function as thermal bridges when the PCM goes through a phase change (such as melting or solidifying), facilitating quick heat transfer and considerably enhancing the material's total thermal conductivity. This improvement makes NePCM useful for applications needing precise temperature control and increased energy efficiency because it leads to more rapid and effective heat absorption or release during phase transitions (Wei et al., 2018).

Mahdi et al., (2019, 2018) separately examined the effects of copper fins and Al_2O_3 nanoparticles in the PCM of a triplex-tube heat exchanger lattice heat-storing unit. The findings demonstrate that fins facilitate a greater PCM fusion rate than nanoparticles in boosting heat transmission. The research also indicated that the fusion rate can be increased by applying extended fins in the bottom half of the field, where conduction predominates in heat transmission. A novel fin arrangement optimised using RSM (Response Surface Method) with the highest energy storage capacity as the goal function was analyzed by Lohrasbi et al. (2016) in computational research utilising the finite element approach. In addition to improved storage conditions, advances in PCM solidification rates were seen when the optimised plan was associated with other fin configurations of the storage unit. Lohrasbi et al. (2017) followed up with research that considered a fin arrangement that might be fitted to the condenser of a thermal pipe that encounters PCM. Based on the entire phase change duration, the research found that a specific fin arrangement worked best for loading and unloading operations.

Different geometric shapes of the cavity and various imposed temperature gradients and cavity topologies have been studied in recent decades. Standard geometric shapes include spheres, squares, rectangles, and triangles (Alshare et al., 2022; Bhatti et al., 2022) as represented in Fig. 1. Many researchers have studied the geometry of primary enclosures for convective heat transmission, including triangles, C-shapes, concentric annuli, hemispheres, and parallelograms (Maneengam et al., 2022). Over the last decade, the subject of thermal analysis in different cavity shapes has been reviewed by a number of scholars.

For the solidification and melting process of NePCM, Irwan et al. (2019) conducted a critical review of numerical simulations. Nanoparticle fraction in the mixture, nanoparticle size, enforced boundary constraints, and container shape were all studied to better understand their effects on the final result. The influence of nanoparticle size and shape was studied far less often than the effect of particle fraction. Comparisons were made between the numerical models used to simulate the numerical activities. The majority of the studies used the enthalpy-porosity formulation in conjunction with the finite volume approach. Rather than trying to represent NePCM as a two-phase material, which necessitates a multi-domain approach, most models have only addressed a single macroscale domain at each iteration by assuming it is a single-phase substance. When the mesoscale approach (the Lattice Boltzmann approach - LBM) is used, this problem is avoided.

NePCM were presented by Dhaidan et al. (2022), who reviewed the experimental, computational, and analytical research on the solidification of NePCM in typical containers used for TES, including planar, spherical, annular, and cylindrical enclosures. Wall waviness, thermal radiation, magnetic field strength, temperature, heat transfer fluid (HTF) flow rate, and nanoparticle dispersion were all considered and weighed against one another. The findings demonstrated that the thermal conductivity of NePCM can be enhanced by the incorporation of the NePCM matrix. As a result, NePCM has a faster solidification rate and a shorter freezing time than pure PCM. The ability of NePCM to store energy is reduced, however, when nanoparticles are presented. Increasing the HTF flow rate, reducing the HTF temperature, or doing both, may also enhance the freezing qualities.

Xiong et al. (2020) provided a comprehensive review of the current numerical research on NePCMs for TES. Results from these simulations were mainly reliant on single-phase techniques and prediction models of effective thermo-physical properties. Then, the concepts of NePCMs' melting and hardening in different geometries, including holes, tubes, cylinders, spheres, and annuli were addressed. Also, the topic of heat storage and release performance, and how it varies according to the kind, shape, size, and concentration of nanostructures was discussed thoroughly. The effectiveness of increasing heat transfer by nanoparticle dispersion was compared to that of using fins or porous foams. The discrepancy between simulation and experiment, as well as the reasons behind it, were evaluated critically.

The PCMs and heat-enhancement techniques for PCM storage were examined by Muhammad and Andrzejczyk (2023). Researchers not only detailed recent developments but also offered an overview of PCMs and their potential uses. The authors focused on heat enhancement techniques including extended surfaces, multiple and composite PCMs, and

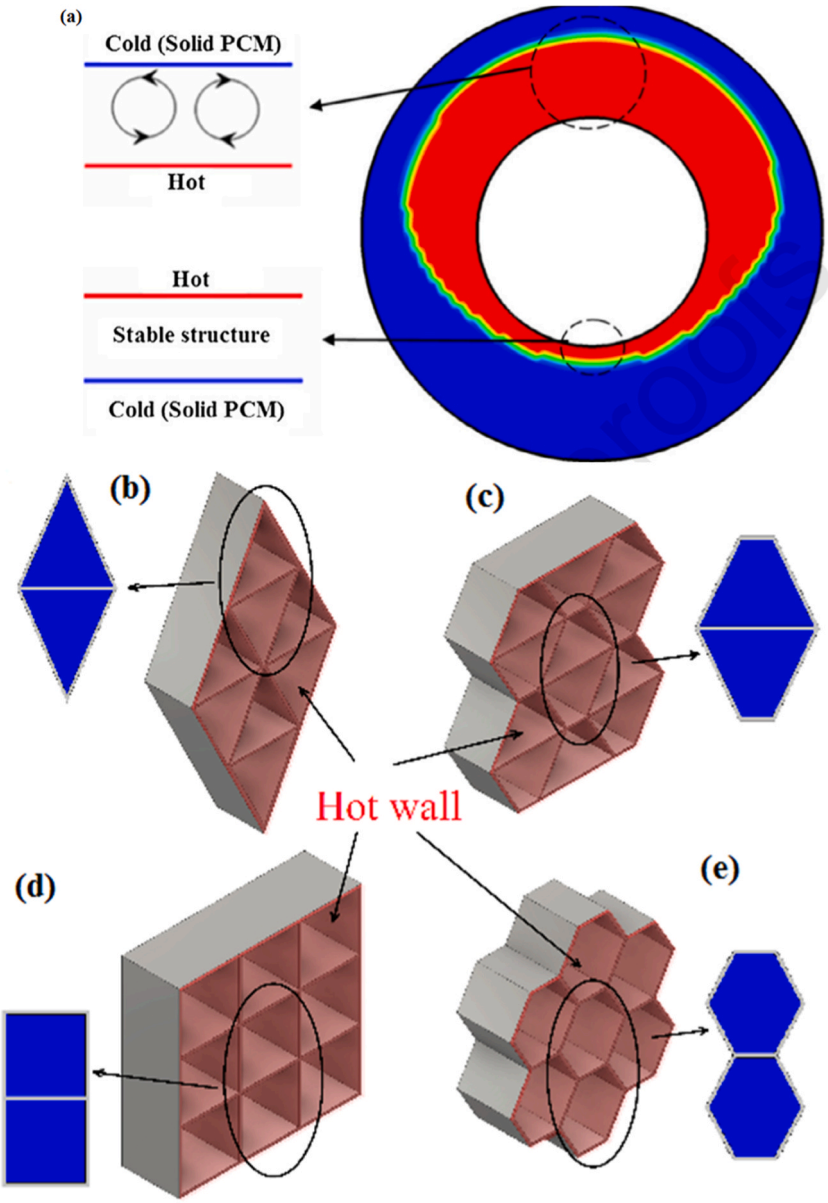

Fig. 1. Sketch of standard geometric shapes of the cavity a) spheres, (b) triangular, (c) trapezoidal, (d) square, and (e) hexagonal (Duan et al., 2019; Xiong et al., 2020).

encapsulating approaches, in addition to providing a statistical overview of studies published between 2016 and 2021. The relevance of various fin and tank forms (extended surfaces) was discussed. It was then admitted that the usage of NePCMs is one of the new techniques explored for improving heat output.

Heat transport evaluations in various geometries, including circular, cylindrical, hexagonal, and rectangular cavities, were reviewed by Rashid et al. (2022b). According to this review, fins improve heat transfer and reduce PCM melting time, while cavity tilt and wind speed determine the best wind occurrence angle for maximal loss of mixed thermal convective. When the Richardson number (Ri) is decreased, the graphs of the Nusselt number (Nu) change their behaviour. At Ri = 10, natural heat transmission is the primary mechanism, but at Ri = 1, lid motion is nonexistent. The blockless cavity outperformed the square and circular block cavities for a given Ri and Pr. It has been determined that the heat transfer coefficient at the heating sources is a useful measure of efficiency. Fins on the heat source speed up the melting process of gallium and increase its efficiency.

Despite the existence of the above review studies, there is no comprehensive overview of heat transfer investigations in the specific set of cavity designs including spheres, squares, trapezoids, and triangles in the existing literature. Therefore, an effort has been undertaken to carry out this analysis. Thus, this paper intends to discuss the associated studies published between 2016 and 2023 to perceive various scientific, research, and advancement strategies for cavity design. A thorough comprehension of the material presented here will facilitate further development and provide a workable answer to various problems. Heat transfer is still an area of action, and this study would shed a light on the differences in progress made for spherical, square, trapezoidal, and triangular cavities. The results of this study might pave the way for similar investigations in the future.

2. Review method

To provide an overview of papers that investigated heat transfer in various cavity geometries including spheres, squares, trapezoids, and triangles with and without NePCMs, a systematic literature review is performed. The review is carried out by conducting a critical analysis of

existing academic literature. Various databases have been used to identify peer-reviewed academic literature, including SpringerLink, ScienceDirect, Google Scholar and Scopus. The keywords for the search included PCM, heat transfer, cavity, heat convection and forced convection. Although there were no stringent restrictions on the publication timeframe, emphasis was placed on prioritizing recent publications between 2016 and 2023 in order to address the recent state-of-the-art research.

2.1. Review of spherical cavity

It is generally agreed that improving heat transmission is one of the most critical challenges in today's power plant engineering. The requirement to provide thermal protection of high-power stressed parts of contemporary thermal power plants (like gas turbine blades and the fuel elements of nuclear power plants) has accelerated the development of this technology. Research on the sphere's cavity is included below.

The experimental technique of inward solidification heat transfer of a PCM contained in spherical capsules was suggested by Liu et al. (2016). A steady infusion of liquid PCM continually compensated for the volume loss. It was simple to reduce other parameters of interest to single-valued functions of the volume contraction, such as the solidification percentage and the surface-averaged heat flow. The suggested approach was realised in the lab using a stainless steel spherical capsule with an inner diameter of around 60 mm and 1-tetradecane as the PCM. Three different border cooling temperatures were tested simultaneously. The heat transmission rate decreases rapidly at the start of solidification. As shown in Fig. 2, the overall solidification time for $\Delta T = 10\ ^{\circ}C$ is around three times that for $\Delta T = 30\ ^{\circ}C$.

One-dimensional wave problems in a thermo-elastic infinite media with a spherical cavity were explored by Lotfy (2017). Using a novel fractional order model, the authors focused on better understanding the heat conduction law in a spherical hollow made from a semiconductor material. The governing equations were solved through a photo-thermal process in the context of the theory of linked plasma, elastic, and thermal waves. The inner wall of the hollow was ripped free of adhesion by applying heat. Applying the Laplace transform method to the governing equations eliminates time dependency. Some physical quantities, such as the parameters of thermal activation coupling, have been visually expressed using this manner.

Using a spherical cavity occupied with a metal foam and a predefined temperature gradient, El-Sapa (2020) studied the impact of the permeability of a Brinkman media on thermophoresis for the quasi-steady transverse movement of a rounded particle placed at the center of the cavity. Fluid flow through a porous media was characterised by a continuum model, including increases in temperature, heat creep, viscous slip, and thermal stress at the solid surfaces of the particle and cavity if the Knudsen number (Kn) is believed to be minimal. An analytical formula for the thermophoretic velocity of the restricted particle was generated for various values of the Brinkman number describing the permeability of the substance, the thermal properties of the porous material and particle, and the particle-to-cavity radius ratio.

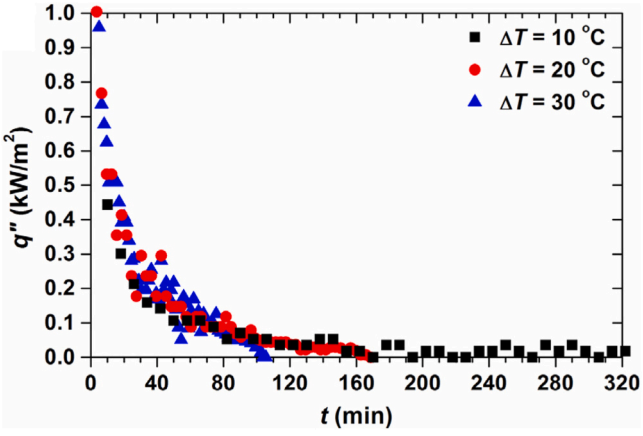

Fig. 2. Time-varying instantaneous surface-averaged heat flux (Liu et al., 2016).

Theoretical research on the quasi-steady thermophoresis of an aerosol sphere situated randomly in a spherical cavity normal to the line of their centers was described by Tseng and Keh (2020). Thermal creep, thermal stress slip, frictional slip, and temperature leap are all allowed on solid surfaces in the slip-flow regime of gas motion. The findings demonstrated the boundary's importance, novelty, and complexity impact on the thermophoretic movement. The analytical answer for the particle's migration speed was in good agreement when the particle was in the cavity's center. There are few exceptions; generally, thermophoretic mobility decreases as the particle and cavity centers' normalized distance and particle-to-cavity size ratio grow. Depending on the cavity's geometry and characteristics, the thermostatic flow induced may either accelerate or slow down the thermophoretic migration and delay or reverse the rotation of the particles. Compared to the boundary effect along the line connecting the centers of the particle and the cavity, the result type to the bar is somewhat smaller.

In the existence of NePCM, Fan et al. (2016) examined the classic issue of unrestrained melting experimentally in a spherical container. Graphite nano-sheet loadings up to 1% by weight were used to create the NePCM samples. The loading and temperature of the NePCM tests were tested in-house to determine various significant thermo-physical parameters. In the melting trials, several boundary temperatures were used. At the minimal boundary temperature (just 8 °C greater than the phase change point), it was shown that the 0.5 wt% sample had a 10% shorter total melting time than pure PCM due to the improved thermal conductivity. It was also thought that the increase in viscosity inside the close-contact melting area would cause the thin molten layer to thicken, preventing heat transfer. All NePCM samples were claimed to have universal correlations with an overall uncertainty of less than 15%.

Natural convection, the transfer of heat from an interior hot body to its outside environment, was studied using three-dimensional numerical simulations by Welhezi et al. (2020). In this hypothetical physical model, a cube-shaped entity occupied the center of an otherwise empty, isothermal sphere. Therefore, the temperature difference between the cooled sphere and the heated cube causes the fluid to flow within the enclosure. The range of descriptive Rayleigh numbers (Ra) used here spans three orders of magnitude, from 10^4 to 10^7, and was covered by the use of three different fluids: air Pr = 0.71), water Pr = 6.2), and a dielectric liquid Pr = 25). Distributions of iso-contours of temperature, iso-surfaces of the standard velocity vector, and stream traces for various Rayleigh numbers were used to analyse the intricate three-dimensional flow and thermal structures inside the enclosure. The total heat transmission characteristics within the chamber were also shown by displaying the fluctuation of the local and surface averaged Nusselt numbers at the inner hot cube wall. It was discovered that for Rayleigh numbers between 10^4 and 10^7, heat and flow fields gradually settle into a steady state. Fig. 3 shows that when the Ra is increased, the thermal rate improves until it reaches its maximum value at Rayleigh number 10^7.

Using a pressure decrease as an input, Morenko (2020) conducted a numerical simulation of a spherical gas cavity collapsing in a liquid. Menter's SST model complements the continuity and momentum equations for describing the dynamics of a viscous compressible fluid in an unstable state. To observe the gas-liquid multiphase flow interface, the VOF method was implemented. The Open FOAM program was used to fix the issue. Keeping the liquid pressure at 7 MPa, the starting radius of the spherical cavity was adjusted in the tests from 0.01 to 0.09 m, while the gas pressure was changed from 0.05 to 0.5 MPa. As shown in Fig. 4, the extreme pressure at the limit point falls consistently with an increase in starting gas pressure and, therefore, lowering Δp. Thus, the

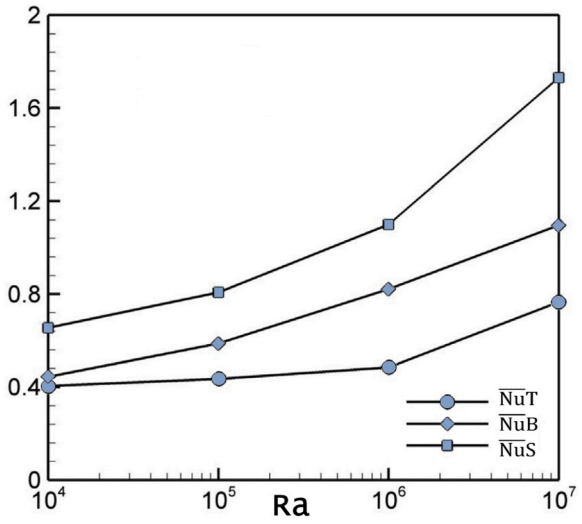

Fig. 3. Rayleigh number variation of averaged Nusselt numbers at the inner cube's top, bottom, and side walls (Welhezi et al., 2020).

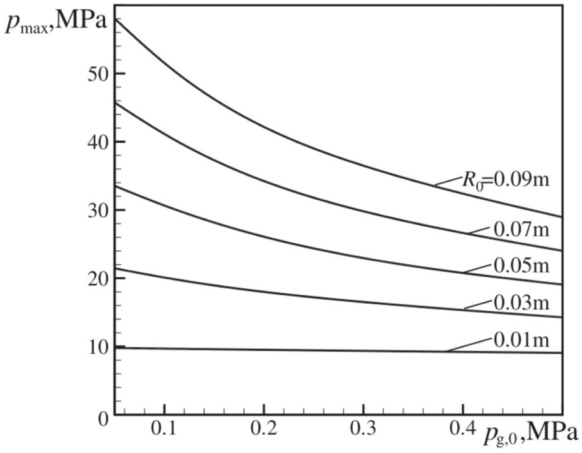

Fig. 4. The greatest pressure observed at the limit point at 0.1016 m from the cavity center depends on the starting gas pressure (p_g,0) for varied gas cavity radius R0 (Morenko, 2020).

maximum pressure at the control point is more significant if the starting radius R0 of the gas cavity is larger and the pressure drop Δp is more prominent at the beginning time.

The discharge method of nanofluids in spherical spaces was the subject of numerical research by de Souza et al. (2020). The model was built by including the process's convective elements by applying the thermal conduction formula in both the solid and liquid phases of the field, with efficient heat conductivity in the liquid phase. Model equations were solved using an implicit discretization technique, and the results were checked against an analytical solution found in the literature to ensure the accuracy of the finite difference approach. Scientists were interested in determining how nanoparticles affect the nanofluid's solidification and liquid phase cooling rates. Water was used as the basis fluid in all four kinds of nanofluids that were studied. Figs. 5 and 6 illustrate that the attendance of nanoparticles in the base fluid speeds up the chilling progression and shortens the time needed for complete solidification.

To store and stabilize thermal energy, Meghari et al. (2021) investigated the use of PCM in passive solar buildings and other applications. A spherical capsule with regular and hollow fins contains the PCM of n-octadecane and Gallium. The effectiveness of a conventional fin vs a

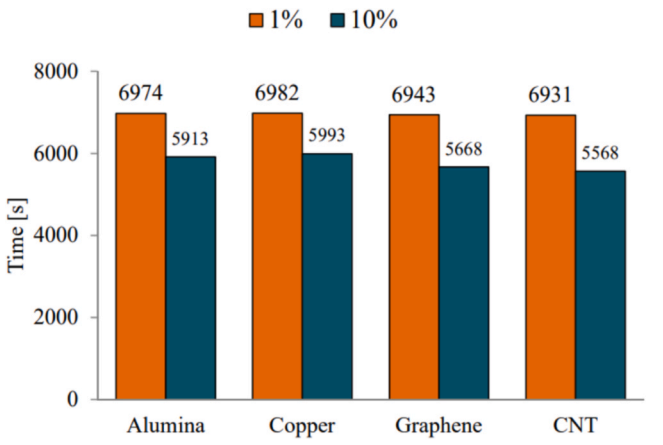

Fig. 5. Alumina, Copper, Graphene, and Carbon Nanotubes total solidification times in water (de Souza et al., 2020).

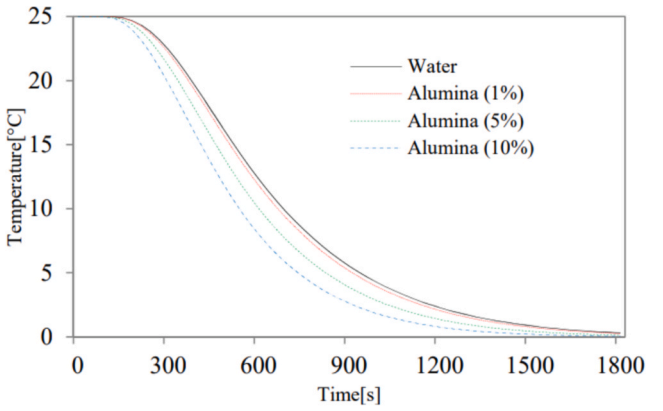

Fig. 6. Liquid-phase cooling and Al_2O_3 nanoparticle concentration (de Souza et al., 2020).

hollow one at varying angles has been simulated using computational fluid dynamics (CFD). For a comprehensive knowledge of the PCM behaviour, the authors additionally realised the temperature changes within the spherical capsule along the horizontal and vertical axes. In the case of PCM with a hollow fin, the melting time was decreased by 14 compared to a configuration without fins.

The linked issue of spherically symmetric elastic-plastic deformation and material heating owing to plastic dissipation, resulting in altered mechanical characteristics, was analytically solved by Sevastyanov (2021). A material's elastic and plastic mechanical parts may have arbitrary temperature dependencies. In this context, the scientists supposed that elastic and plastic deformations are bounded. The effect of temperature on material expansion was disregarded while assuming an adiabatic heating process. Temperature was used as a monotonic independent variable in place of a geographic location. This allowed us to focus on a first-order ODE solution instead of the original issue. Any incompressible hyperelastic solid, whether perfectly-plastic or exhibiting isotropic strain-hardening/softening, may use the derived solution. For the von Mises model, the plastic and elastic stress zones are shown in Fig. 6. At infinity away from the cavity, the stress condition is analogous to that under hydrostatic loading (tension or compression). As shown in Fig. 7, all stress components are negative during a cavity contraction and positive during a cavity expansion.

For the purpose of clarifying the alignments of numerous rigid rods enclosed inside a rigid spherical cavity under crowding, Shew and Yoshikawa (2023) performed a Monte Carlo simulation for a basic model. Depletion forces are required if a rod's length exceeds the

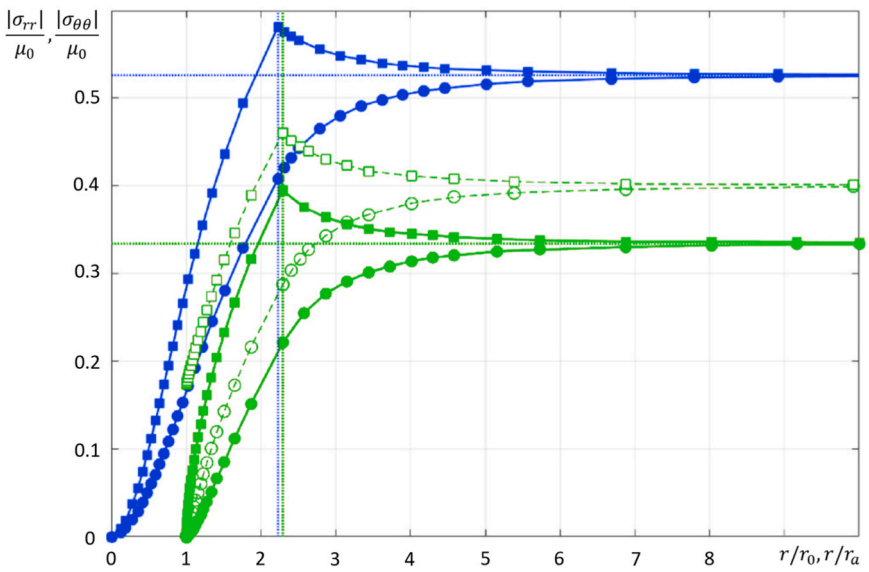

Fig. 7. Stress distribution (von Mises model): The green line shows the steady-state cavity expansion, and the blue line indicates the completely closed cavity under contraction. The dashed line shows the isothermal approximation; the square marker shows the curves $|\sigma_{\theta\theta}|/\mu_0$ and the circle marker shows curves $|\sigma_{rr}|/\mu_0$; the vertical lines show the location of the elastoplastic boundary (Sevastyanov, 2021).

cavity's radius. Low orientation ordering occurs when rods disperse across the cavity perimeter in the presence of stiff crowders. Crowding causes rods longer than the cavity's radius to form a bundle within the cavity and exhibit nematic ordering. Due to the entropic benefits of nematic order formation, crowders have more room to distribute along the cavity border.

Jiao et al. (2023) detailed a firmly mounted, vibration-insensitive, multi-tubes, portable spherical optical reference cavity. The design was based on a spherical shape, with the four proofs placed in a symmetrical tetrahedral array around the optical axis. Researchers performed theoretical calculations to determine how sensitive the multi-tube cavernous visual reference structure is to vibrations. Researchers employed a straightforward technique to test the vibration sensitivity of the spherical visual reference cavity by monitoring the shift in line with the produced by vibration in the cavity. The optical reference cavity has an acceleration sensitivity of about (5.1–8.4) 10^{-10}/g for vibrations in all three directions. The cavernous visual reference structure has nearly half the mass of a significant visual reference structure of the same size, although it is more sensitive to vibrations.

The non-self-similar growth of a spherical hollow in a drained elastic-plastic soil mass of limited radial extent was studied again by Yang et al. (2023). They deployed several well-known soil models to analyse this issue and construct rigorous semi-analytical solutions. Considering the stress dependence of soil moduli and the impacts of the outer boundary, analytical equations were produced for elastic stresses and displacements under the minor strain assumption. In the plastic zone, a novel combination of the Lagrangian and Eulerian descriptions was used to define a set of first-order partial differential equations (PDEs), and an effective method for solving these equations is devised. It was shown that the border effect may significantly impact the cavity expansion response when the ratio of the outside to the inner radius is minimal. Table 1 presents a summary of the conducted studies of spherical cavities.

2.2. Review of square cavity

Nanotechnology has quickly risen to prominence as one of the cutting-edge fields of study. Heat transfer has several applications in technology, including computer and nuclear reactor cooling, heating, solar thermal power generation, solar thermal power production using flat panel collectors and micro-channels, and entropy generation using solar thermal power generation. Heat transport from electronic circuits has been studied extensively since the development of supercomputers and electronic microchips. Due to their enormous heat output, such devices seldom have enough ventilation. Studies using a square cavity are discussed here.

The effects of suction/injection zones, Brownian diffusion, and thermophoresis on mixed convection in a porous square cavity were investigated by Sheremet et al. (2018). High-concentration nanofluid flows into the hollow via its open bottom border and leaves through its open top section. The inflow boundary conditions were applied to the upper wall of the open cavity, where the nanofluid concentration is high, the temperature is low, and the vertical velocity is constant. The assumptions of an isothermal vertical wall and an adiabatic horizontal wall were made. Modifying the Rayleigh numbers, unnumbered Thermophoresis, in which nanoparticles move from the heated wall to the cold nanofluid flow, was amplified as the Reynolds number increased. Increasing the inlet and exit diameters caused a significant cooling of the cavity and a less significant reduction in the volume fraction of the nanoparticles in the top left corner.

For the issue of natural convection heat transfer in a square cavity, Wang and Qin (2018) created a Legendre spectral component design of an enhanced time-splitting approach. Different treatments were given to the convection heat, the Stokes term, and the temperature diffusion part. The convection and dispersion of temperature terms were solved using the usual Galerkin difference, while the Stokes term was solved using the least-squares variation owing to the inf-sup constraint. Since the original time-splitting approach no longer makes intermediate velocity and pressure assumptions, the resulting velocity was entirely divergence-free. The numerical test confirms the verification and h-p convergence properties of this approach. Additionally, numerical solutions were found that match well with both current computational and experimental data for natural convection heat transfer in a square cavity with a Rayleigh number in the range of 10^3–10^6. The heat conduction at S1 and S2 is better than that around S3 and S4. As shown in Fig. 8, an improvement in the Ra improves heat transmission close to the heat sources, except in the top left corner of S1 and the upper and leftward side of S4.

Using a rectangular chamber filled with nanofluids, Solomon et al. (2017) conducted experimental research on the effect of the Aspect Ratio (AR) on natural convection. The heat transfer performance of

Table 1
Studies outline spherical cavities.

Authors (year)	Structure	Examined variables	Study method	Results / Impacts
Liu et al. (2016)	PCM is enclosed in spherical capsules.	Effect of sub-cooling degree.	Experimental	The total solidification time for $\Delta T = 10\ ^{\circ}C$ is about 3 times longer than that for $\Delta T = 30\ ^{\circ}C$.
Lotfy (2017)	Thermo-elastic infinite medium with a spherical cavity.	Effect of coupling thermo-elastic parameter, associating thermoelectric parameter, and fractional order.	Numerical	A discernible influence of the thermo-elastic coupling parameter may be seen within this range. When the thermo-elastic coupling parameter is increased, this impact becomes less pronounced. When the values of the thermoelectric coupling parameter are raised, the carrier density distribution and displacement distribution amplitude become denser. The influence of the fractional order parameter is significant for the study of physical fields.
El-Sapa (2020)	A temperature gradient is applied, and a spherical particle is placed in the middle of a spherical cavity with porous media. This causes the particle to move in a quasi-steady translational motion.	The impact of a Brinkman porous media on thermophoresis.	Numerical	The non-dimensional velocity falls when the permeability parameter and the particle-to-cavity radius ratio increase.
Tseng and Keh (2020)	Thermophoresis of an aerosol sphere that is quasi-steady and is situated randomly in a spherical cavity in an average direction to the line that runs between their centers.	Effect of particle-to-cavity size ratio and the circulating cavity-induced thermostatic flow.	Numerical	The particle-to-cavity size ratio and the normalized distance between the centers of the particle and cavity both have a negative impact on thermophoretic mobility; however, there are rare instances when this is not the case. The circulating cavity may accelerate or reduce the thermophoretic migration, and it can slow particle rotation. The circulating cavity causes the thermostatic flow.
Fan et al. (2016)	The classic issue is unrestricted melting inside a spherical container when NePCM are presented.	The weight percent of NePCM	Experimental	For the sample containing 0.5 wt percent at the minimal boundary temperature (8°C greater than the phase change point), the melting time is reduced by 10%.
Welhezi et al. (2020)	The natural convection events that take place between a heated body's interior and its surrounding enclosure.	Effect of Rayleigh numbers.	Numerical	The best heat transmission rate may be achieved by setting the Rayleigh number to 10^7 and raising it until it reaches its maximum value. The heat transfer rate increases dramatically as the Rayleigh number increases.
Morenko (2020)	The collapse of a spherical gas cavity inside a liquid result from a decrease in pressure.	Effect of initial gas pressure and initial radius.	Numerical	The extreme pressure value at the control point consistently declines due to the growing starting gas pressure and, as a direct consequence, the lowering p-value. If the starting radius R0 of the gas cavity is bigger and the pressure drop at the beginning time is greater, then the control point's maximum pressure will likewise be higher.
de Souza et al. (2020)	A procedure for the solidification of nanofluids inside spherical cavities.	The impact of nanoparticles on the rate at which the liquid phase cools down and the time it takes for the nanofluid to solidify.	Numerical	Incorporating nanoparticles into the base fluid has been shown to speed up the cooling process and shorten the time necessary for complete solidification.
Meghari et al. (2021)	A spherical capsule containing a PCM of n-octadecane and gallium, having both standard and hollow fins.	Effect of fins on the melting time.	Numerical	Compared to a configuration with no fins, the PCM configuration with hollow fins has a melting time that is 14 times faster than the configuration without fins.
Sevastyanov (2021)	The linked issue of spherically symmetric elastic-plastic deformation while, at the same time, the material is heating up as a result of the plastic dissipation.	Effect of contraction and expansion in the cavity.	Numerical	When the cavity contracts, all of the stress components have a negative sign, but when it expands, they all have a positive sign.
Shew and Yoshikawa (2023)	Multiple rigid rods are crammed into a single rigid spherical cavity, which results in crowding.	Effect of rigid rods.	Numerical	Entropically speaking, forming a nematic order is preferable, increasing the open space available for crowders to distribute around the cavity border.
Jiao et al. (2023)	The sphere shape with 4 proves organized symmetrically in a tetrahedral arrangement around the optical axis of the sphere.	Effect of cavity geometry.	Experimental and Numerical	The spherical optical reference domain has a volume nearly equal to 1/2 that of a cubic optical reference cavity with the exact dimensions, despite having a greater vibration sensitivity than a cubic visual reference cavity.
Yang et al. (2023)	A spherical hollow inside anelastic–plastic soil mass with a limited radial extent under the drained circumstances.	Effect of the ratio of the outer to internal radius.	Numerical	When the ratio of the external to the internal radius is low, the boundary impact has the potential to have a considerable effect on the expansion response of the cavity.

de-ionized water and Al_2O_3/Water nanofluids was investigated in three distinct cavities with 1, 2, and 4 AR values. The Nusselt number and heat transfer coefficient was shown to be significantly impacted by the cavity's AR. However, the AR of the cavity affects the ideal nanofluid concentration for maximal heat transmission. The study also discovered that the Rayleigh number strongly influences the Nusselt number and the buoyancy of nanofluids.

Natural convection was studied by Haq et al. (2020) using the finite

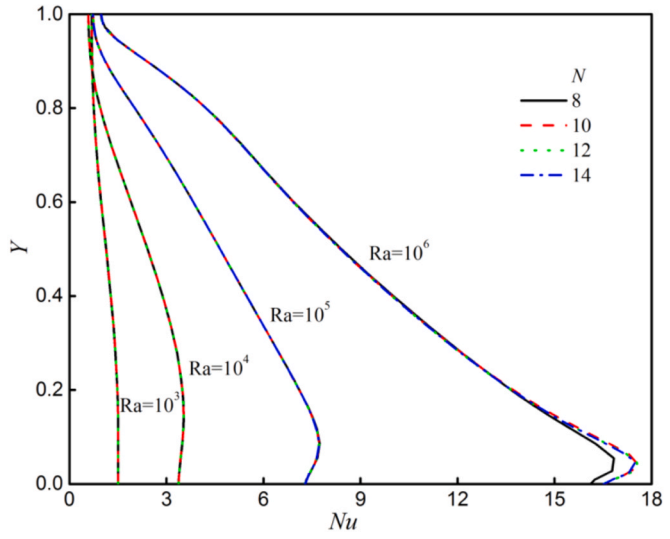

Fig. 8. Local Nu on the heated wall at various interruption orders and Ra(s) (Wang and Qin, 2018).

element method (FEM) in a square cavity occupied with water-based Single Wall Carbon Nanotubes (SWCNTs). There were additionally three parallel vertical fins and one horizontal fin at the top positioned inside the hollow. While the top surface of the square cavity was adiabatic, the other three sides were chilly. Lower horizontal and centrally heated fins promote convection. New characteristics such the Ra, nanoparticle loading (ϕ), heated flat fin location, bottom heated fin length variation (HT), Hartmann number (Ha), and center vertical fin effect (adiabatic, cold, hot) were considered to produce results for temperature profile and stream function. Increasing the heated length of the lower horizontal fin improves the heat transfer rate, whereas increasing the value of Ra and the solid volume percentage of nanoparticles reduces it, as shown in Fig. 9.

A novel lattice Boltzmann method (LBM) was developed by Chen et al. (2018), and three independent benchmarks have verified it. An open-ended porous-partially-filled square cavity was studied using the LBM to determine the effects of porous layer thickness, fluid-to-porous thermal conductivity ratio, and permeability on conjugate natural convection heat transfer. It was discovered that these parameters have a significant impact on the flow field and temperature field patterns. In particular, there were certain essential thresholds. If you move them a little, the heat and mass transmission will completely differ. Sometimes established patterns of change suddenly reverse. A more breathable porous layer would lead to a less uniform heat transmission rate. Heat transmission is greatest at the hot wall's top half of the highly permeable porous layer (Da=10^{-3}). Heat transfer intensity, however, decreases monotonically with increasing distance from the hot wall for a porous layer with low permeability (e.g., Da=10^{-5}), as shown in Fig. 10.

Alnaqi et al. (2019) used a diagonal square cavity with a conductor fin to quantitatively examine the impact of magnetic flux and radiation on entropy generation in nanofluids and the rate of thermal convection. A fin has a k * = 100 heat conductivity coefficient on one of the cavity's walls. The fluid was assumed to contain a volumetric thermal source responsible for heat emission. The radiation parameter (Rd) represents the influence of this source when it is included as a source in the energy equation. This research examined the relationship between the Rayleigh number, the Hartmann number, the radiation parameter, and the nanoparticle volume fraction on entropy formation and heat transmission. According to the findings, the Nusselt number rises as the Rayleigh number and falls as the Hartmann number. Heat transfer increases by 5.9%, and entropy formation rises by 16.6% when 6% of the nanoparticles are added to the base fluid without radiation. Radiation parameter Rd = 3 and nanoparticle volume fraction of 6% contribute to an expand of 3.4% in thermal rate and 11.2% in total entropy production, respectively. Fig. 11 shows that the local Nusselt numbers rise with increasing radiation factors.

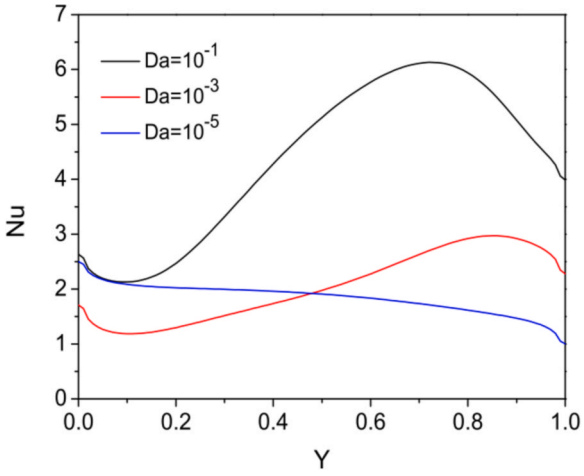

Fig. 10. Local Nusselt number along the hot wall at various Da (Chen et al., 2018).

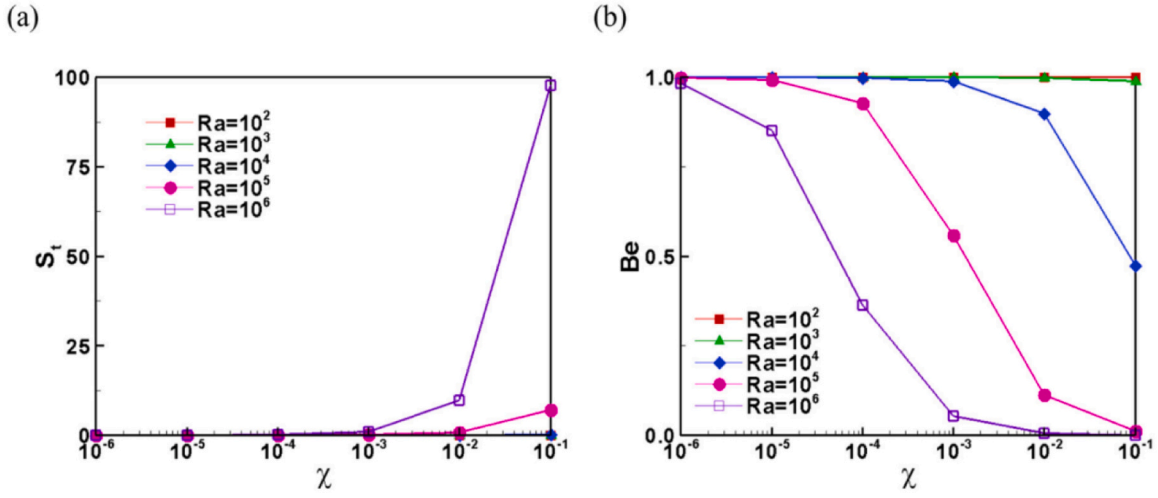

Fig. 9. Variation of (a) S_t and (b) Be with χ as a function of Ra (Cho, 2020).

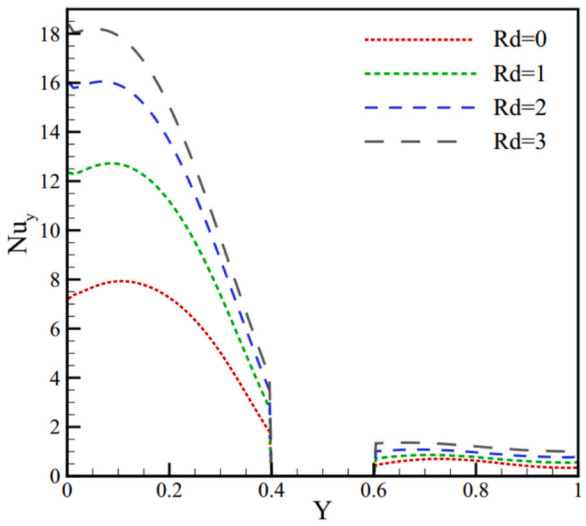

Fig. 11. The local Nu for fixed values of Ra= 10^5, Ha= 20, φ = 0.03 and various radiation variables on the heated wall of the cavity (Alnaqi et al., 2019).

Semi-analytical formulations of the incoming radiation and radiative flux fields were established by Djeumegni et al. (2020) within a two-dimensional semi-transparent material, and then numerical simulations were performed. A grey absorbing-emitting, non-scattering, semi-transparent medium fills a rectangular cavity at radiative equilibrium. Although the inside of a black, temperature-controlled cavity at the hollow's center was treated as a non-contributing medium, the cavity's boundary surfaces nonetheless contribute to radiative transmission. The incident radiation and radiative flux fields were calculated using an accurate technique based on ray tracing and specialized algorithms. Radiation blockage affects the path of hot particles and changes the anticipated radiative amount. Optical thickness has a role in the rapid cooling of a medium.

A numerical study of convective-radiative heat transfer in a rotating square cavity with a locally generated and conducted heat source was given by Mikhailenko et al. (2018). The suggested cavity contains a heat-generating unit on the bottom wall and horizontal adiabatic walls on the top and bottom. Non-dimensional stream function, vorticity, and temperature mathematical models have been solved using the finite difference approach. Streamlines, isotherms, the average Nusselt number, the flow rate, and the average temperature within the heater have all been analysed to see how they change depending on surface emissivity, Taylor number, and Ostrogradsky number. After many rotations, it has been observed that heat-generating and heat-conducting elements exhibit periodicity in the intensity of their fluid flows and the rates at which they transmit heat. The average temperature within the heated part may be lowered by increasing the surface emissivity or by spinning the element rapidly.

Using numerical simulations, Javed and Siddiqui (2018) investigated the effect of an external magnetic field on free convection heat transfer in a water-based ferrofluid flowing through a square cavity with a heated square blockage of varying aspect ratios ($0 \leq A/H \leq 0.5$). They assumed the enclosure has insulated walls at its vertical bounds and that the bottom horizontal wall will be evenly heated while the flat top border will be consistently cooled. The cavity's central square obstruction is both a thermal mass and a potential safety hazard. Nonlinear partial differential equations (PDEs) represented the mathematical model, and the Galerkin finite element technique was used to solve them. The outcomes were shown across broad physical parameters, including Rayleigh, Prandtl, and Hartmann numbers. It was found that the heat and flow structures are susceptible to the magnetic field intensity, Rayleigh number, and ferroparticle concentration in the base fluid.

An open square-cavity solar receiver was the subject of a computational and experimental heat transport investigation by Alvarado-Juárez et al. (2020). The Rayleigh numbers (Ra) 10^4, 10^5, and 10^6 were used in the numerical analysis, which modelled laminar flow in an open square cavity. The research considered transparent and radiatively participating material for radiative heat transfer. Differences between the two scenarios highlighted the need to view a radiatively participating material. Fig. 12 depicts the development of a temperature measurement made at two different distances from the center of the receiver plate (r = 0 cm and r = 2.0 cm). Both temperatures are 30 °C at the start of the experiment. The chamber heats up to around 540 °C when a beam of concentrated solar light hits it.

Numerically conjugate heat transfer of incompressible laminar flow was investigated by Mohebbi et al. (2020) using the lattice Boltzmann method (LBM) within a two-dimensional chamber with two vertical conductive partitions. Water- (Al_2O_3) nanofluid has been pumped into the chamber. Using streamlines, isotherms, and the mean Nusselt number, we have studied the nanofluid's hydrodynamic and thermal behaviour in the presence of rectangular partitions. This simulation demonstrated rectangular chambers' impact on the velocity, temperature, and heat transfer rate. As the Rayleigh number increased from 10^3 to 10^6, and the nanofluid volume percentage rose from 0 to 0.05, the average Nusselt number also rose linearly. Testing with various partition height/thickness ratios showed that the heat transmission rate may be improved.

Natural convection heat transfer of low turbulence flow of Al_2O_3-water nanofluid within a square cavity was simulated using a computational model developed by Azimikivi et al. (2020) to account for the impacts of rib form with constant height, breadth, pitch, and nanoparticle diameter. The top and bottom walls were insulated, and there were two ribbed vertical walls whose temperatures were kept at different constants ($T_H > T_C$). The effect of Rayleigh numbers 10^7, 10^8, and 10^9 on the heat transfer of a nanofluid in a ribbed square cavity with Prandtl numbers 7.0659, 7.3593, and 7.8353 was studied. The effects of volume fractions between 1% and 3% on the CFD simulation of an Al_2O_3-water nanofluid were investigated. The results showed that with a high Rayleigh number, the trapezoidal rib performed the best with a low volume fraction. Additionally, both N_{BT} (Brownian diffusion ratio to Thermophoresis diffusion) and nanofluid heat transfer benefit greatly from a decrease in nanoparticle diameter. However, when the nanoparticles' size increases, the convection heat transfer efficiency drops below that of the base fluid and smooth walls.

Within the range of the Rayleigh number from 10^3 to 10^8, the thermal conductivity ratio of the partition to that of the fluid from 0.1 to 1000, and the dimensionless partition thickness from 0.05 to 0.2, Khatamifar et al. (2021) numerically studied the transient conjugate natural

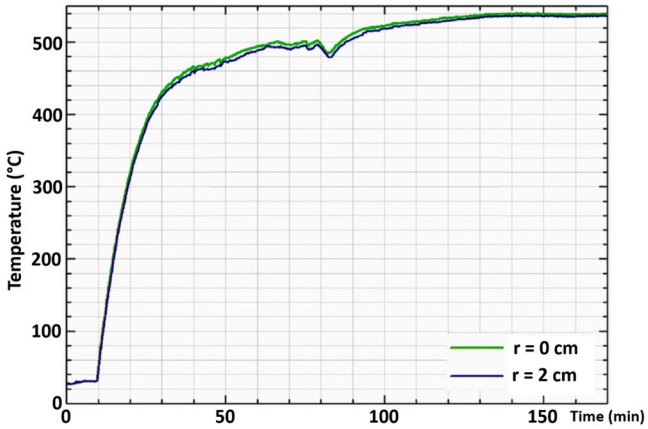

Fig. 12. Evolution of the temperature at the receptor plate (Alvarado-Juárez et al., 2020).

convection heat transfer in a differentially-heated cavity with a partition of finite thickness and thermal conductivity. The effect of the thermal conductivity ratio on the obtained temperature contours and profiles, the time for the onset of stratification, and the Nusselt number becomes negligible as the thermal conductivity ratio becomes very large (100 or beyond), as shown by an analysis of these variables. Partitioned cavities were consistent with the scaling equations established for the un-partitioned cavity. The findings also demonstrated that the partition thickness has a noticeable impact on heat transmission, especially in cases when the ratio of thermal conductivities is low.

To find answers to questions about buoyancy-driven flow in a square cavity, Momoniat et al. (2023) used the finite element approach. In their analyses, the team considered scenarios in which there was neither an extended surface nor an adjacent wall, an extended surface nor an adjacent wall, but also the cold wall itself. The Boussinesq and heat transfer equations need some degree of artificial diffusion to get stable numerical solutions, which a study of the P é clet number may estimate. Specifically, they looked at how the characteristic length influences the flow in the square cavity. The researchers demonstrated grid convergence by calculating the grid convergence index (GCI). The results indicated that the flow is reduced by 31% and 33% for cases with two and three extended surfaces, respectively, when insulated boundary conditions are on the sidewalls.

Nanoparticle form influences on nanofluid flow in a lid-driven square cavity with a fixed circular obstruction in the center were described in detail by Rashid et al. (2023d). There was an adiabatic motion along the upper wall of the square hollow. Only the bottom and inside of the circular chamber were heated; the outside walls remained chilly. The diamond-water nanofluid included spherical, columnar, and laminar (non-spherical) nanoparticles. Coupled partial differential equations regulated the modelled flow phenomenon, and these equations were solved using the finite element method (FEM). The graphs show that the nanoparticles with a Lamina (non-spherical) shape perform better in temperature distribution and heat transmission in a diamond-water system.

Using a 2D square cavity PCM with a constant heat flux (60 W) at the left wall/bottom wall, Xie and Wu (2023) simulated the melting process of PCM with varying square cavity aspect ratios. A novel and effective indicator was proposed to disclose the charging rate and conventional phase shift features: the differential liquid fraction curve, which considered the development of the solid-liquid interface. The findings revealed that the total melting time rises as the aspect ratio (AR) increases for both left and bottom wall heating settings. Underside wall warming generally has a more effective charging rate than leftward wall heating, particularly for the cavity with an AR of more than 1. At the highest point of the differential liquid fraction curve, where the longest solid-liquid interface can be seen, the melting rate will be at its highest during the phase transition process. In addition, the "scouring effect" of free convection on the solid-liquid interface would cause the charging pattern of the high AR cavity to resemble the low AR scenario towards the end of the left wall heating phase. Table 2 presents a summary of the conducted studies that outline square cavities.

2.3. Review of trapezoidal cavity

Heat transfer in structures and rooms, thermal control of nuclear reactors, crystal formation, etc., all benefit from understanding how natural convection in cavities works. Such situations include, for instance, insulated strips in the open cavity of solar thermal receivers, the heating and cooling of rooms, the convection and radiation of heat inside spaces, the expansion of heat exchanger surfaces, the construction of structures, and the cooling of electronic components. The research on the trapezoidal cavity is presented here.

A two-dimensional flow study of an isosceles trapezoid cavity was performed by Ibrahim and Hirpho (2021). The trapezium has adiabatic sides because they are not parallel. The bottom wall was subjected to a sinusoidal fluctuating temperature while the top wall remained constant. The cavity's upper wall traveled at a speed of η_0 in the positive x direction. In addition, the Newtonian fluid was assumed to be inert, and the magnetic field intensity, B_0, was fixed constant along the x-axis.Ha = 50, Ri = 0.1, 1, 10,Re = 100, and m = 0.25, 0.5, 1 were the values of the magnetic field parameter, Ri, and Re, respectively, and the amplitude of the sinusoidal temperature, respectively. They can examine the effects of various leading factors by showing streamlines for the flow fields and isotherm contours for the flow temperature. The average Nusselt number for the cavity's upper and lower surfaces changed according to Ha and Ri. The average Nusselt number for both characters rise as the Ri rises. Fig. 13 shows that when the Ha grows from 0 to 50, the average Nusselt number decreases monotonically.

Trapezoidal chambers and oval pins with and without slots were presented in a novel design of plate-fin microchannel heat sinks (MCHS) by Alfellag et al. (2019). Characteristics of thermo-fluid were quantitatively examined and analysed for Re between 100 and 1200. The three geometric characteristics considered are the thickness of the pins' two slanted slots, the pins' distance from the cavity's center, and the pins' overall aspect ratio. The SIMPLE algorithm was used for the calculations, and the governing equations were solved using the finite volume method (FVM). The findings showed that the suggested design works best with the following parameters: AR = 1.25, x = 0.03 mm, and t = 0.008 mm for the pin aspect ratio, pin distance from the cavity center, and slot thickness, respectively, yielding a maximum PEC of 1.37.

Plate microchannel heat exchangers (MHXs) with isosceles trapezoidal reentrant cavities (ITRCs) were developed by Pan et al. (2018). Numerical analysis based on the commercial program FLUENT was used to evaluate the MHX's flow, heat transfer, and pressure drop properties to those of a conventional rectangular MHX. Based on the data, it seemed that when the flow rate increases, both MHXs' heat transfer capabilities improve briefly before declining. The benefit of the MHX with ITRCs in terms of heat transfer performance becomes more apparent at higher flow rates compared to the conventional rectangular MHX. In contrast to the traditional rectangular MHX, the pressure drop is less for the MHX with ITRCs at flow rates of more than 130 ml/min. At the optimal value of the number or height (as indicated in Fig. 14) of the ITRCs, the greatest heat transmission performance is shown. Heat transfer efficiency drops as the degree of synchronicity between the ITRCs rises. Flow rates larger than 60 ml/min favour the from-sparse-to-dense (FSTD) ITRC distribution, whereas lower flow rates favour the from-dense-to-sparse (FDTS) ITRC distribution for heat transmission.

Nayak et al. (2018) utilised a computational method to examine the amount of energy lost in a trapezoidal solar cooker due to convection and radiation. They calculated heat loss from the top glass cover owing to forced convection and radiation. 78% of the total heat loss was attributed to radiation leaving the cavity. Variations in cavity depth, heat transfer coefficients dependent on wind speed above the glass surface, and plate emissivity were used to conduct parametric analyses of heat loss from the cavity. The cavity's flow pattern and isotherms have been analysed using various characteristics. A connection between the overall average Nusselt number and its influencing factors has been created for the solar cooker cavity under consideration, and the results were produced in non-dimensional forms for more general usage.

Heat transmission and loss in the trapezoidal cavity of the linear Fresnel reflector were studied by Dabiri et al. (2018). The calculations assumed the air density within the cavity varies with temperature and in a laminar, steady-state model. Different models were used to assess the impact of the cavity angle and the impact of the tube size. The simulation used the DTRM radiation model and considered radiation, conduction, and convection as boundary conditions for the heat transfer processes. Finally, as it is shown in Fig. 15, raising the cavity angle increases the overall value for heat transfer rate while decreasing the heat absorbed by each tube. Heat transfer rate is also shown to be

Table 2
Studies outline square cavities.

Authors (year)	Structure	Examined variables	Study method	Results / Impacts
Sheremet et al. (2018)	A square-shaped porous chamber filled with a nanofluid based on water and subjected to the effects of suction and injection zones.	Reynolds number and the sizes of inlet and outlet characterizes.	Numerical	An increase in the Reynolds number causes an increase in the necessary cooling of the cavity and an intensification of the thermophoretic process that occurs when nanoparticles move from the warm wall to the cold nanofluid flow. An essential cooling of the cavity is characterized by an increase in the diameters of the inlet and outflow, with a less essential reduction in the volume fraction of nanoparticles in the upper left corner.
Wang and Qin (2018)	A difficulty with heat transmission caused by natural convection was found in a square cavity.	Impact of heat sources.	Numerical	Heat transmission is more effective near S1 and S2 than S3 and S4. The heat transmission rate increases in areas close to heat sources when the Rayleigh number is increased, except in the upper left corner of S1 and the top and left sides of S4.
Solomon et al. (2017)	A chamber in the shape of a rectangle that is filled with nanofluids.	The impact of AR and nanofluid loading.	Experimental	The cavity's acoustic response, or AR, significantly impacts the heat transfer coefficient and Nusselt number. Additionally, the AR of the cavity affects the optimal nanofluid concentration for maximal heat transmission, and this optimal concentration varies from case to case.
Haq et al. (2020)	A square cavity supplied with SWCNTs may have a number of different placements of heated bottom fins.	Effect of heated length of the lower horizontal fin, Ra, and nanoparticles concentrations.	Numerical	Increasing the heated length of the lower horizontal fin will result in a higher heat transfer rate, whereas increasing the value of Ra and the solid volume percentage of nanoparticles will result in a lower heat transfer rate.
Cho (2020)	Nanofluid is inside a porous hollow with wavy walls on both the bottom and the higher levels. The vertical wall is partly heated.	The effects of the Ra, Da, porosity (ε), φ, amplitude of wavy surface (αw), length of partially heated wall surface (L_H*), and irreversibility distribution ratio (χ) on the Bejan number (Be), total entropy generation (St), Nu_m, and dispersion of the energy flow.	Numerical	Thermal convection predominates since the energy flue has formed flow zones with high Da and Ra values. As a result, Be decreases as Ra and Da grow, whereas Num and St both increase. Since conduction heat transfer predominates at low values of Da and Ra, the effects of Da, Ra, and on Nu_m and St are negligible, and Be concepts unity.
Chen et al. (2018)	A square opening that is permeable and only partly filled with material.	The effects of the thickness of the porous layer, fluid-to-porous thermal conductivity ratio and permeability of the porous layer.	Numerical	The top half of the hot wall exhibits the highest heat transmission rate, which is the wall's maximal potential. On the other hand, if the porous layer has low permeability (for example, $Da=10^{-5}$), the heat transfer intensity will gradually decrease as the height of the hot wall increases.
Alnaqi et al. (2019)	Cavity with a diagonal square shape and a conductor fin.	The effects of Ra, Ha, Heat transport and entropy production are influenced by radiation factor and nanoparticle loading.	Numerical	The heat transfer rate and the total entropy production rose by 3.4% and 11.2%, respectively, with the addition of the radiation parameter with the value Rd = 3 and the volume percentage of nanoparticles set at 6%. Increasing the radiation parameter at high Rayleigh numbers also boosted the Nusselt number and entropy production while reducing the Bejan number.
Djeumegni et al. (2020)	A grey absorbing-emitting material fills in the hollow of a rectangular shape.	The effect of blockage of radiation.	Numerical	Because of the impact of radiation blocking, the path of hot particles is altered, and the magnitude of the predicted radiative amount is changed. The speed at which the medium cools down accelerates in direct proportion to the magnitude of the optical thickness.
Mikhailenko et al. (2018)	A locally generated and locally conducted heat source is contained inside a rotating square cavity.	The influence of surface emissivity, Taylor number, and Ostrogradsky number.	Numerical	The average temperature within the heated element may be effectively lowered by increasing the surface emissivity, and this temperature can also be reduced by intensifying the rotation.
Javed and Siddiqui (2018)	When a square blockage is heated, the cavity is filled with a ferrofluid based on water. The aspect ratios of the blockage vary.	Effect of MHD on heat transfer through ferrofluid inside a square cavity.	Numerical	The intensity of the magnetic field, the Rayleigh number, and the concentration of microparticles present in the base fluid are vital factors that influence the heat and flow structures.
Alvarado-Juárez et al. (2020)	Solar receiver with open cavities in a square configuration.	Effect of solar radiation.	Experimental and Numerical	The hole's temperature grows to 540 °C if intense sunlight penetrates it.
Mohebbi et al. (2020)	A hollow that is two-dimensional and has two conducting barriers that are vertical.	The impact of the location and aspect ratio of divisions on the top and bottom walls.	Numerical	As a result of the investigation into various ratios of partitions, it has been shown that the heat transmission rate may be increased by

(*continued on next page*)

Table 2 (*continued*)

Authors (year)	Structure	Examined variables	Study method	Results / Impacts
				reducing the ratio between the height and the thickness of the partition.
Azimikivi et al. (2020)	A nanofluid composed of Al_2O_3-water and housed within a square cavity.	The effect of the various nanoparticle diameters, Rayleigh number, volume fraction, and rib shape.	Experimental and Numerical	When the diameter of the nanoparticles is increased, the amount of heat transferred by convection drops dramatically, falling below that of the base fluid and smooth walls. A low-volume fraction performs better when the Ra is large, and the trapezoidal rib is the most effective.
Khatamifar et al. (2021)	A cavity is heated differently on each side thanks to a partition with a limited thickness and thermally conductive.	The effect of the partition thickness.	Numerical	The thermal conductivity ratio is most likely to be low in situations in which the influence of the partition thickness on heat transmission will be considerable.
Momoniat et al. (2023)	Flow that is driven by buoyancy in a square cavity.	Effect of insulated boundary and extended surfaces.	Numerical	When there are two or three extended surfaces, the situation with insulated boundary conditions on the sidewalls results in a flux reduction of 31% and 33%, respectively.
Rashid et al. (2023)	A square hollow driven by its lid, with a circular obstruction set in the middle.	Effect of nanoparticle shape.	Numerical	The nanoparticles with a lamina shape (a shape that is not spherical) perform better in terms of temperature distribution and heat transmission in diamond-water systems.
Xie and Wu (2023)	Under the assumption that the heat flow remains the same, several aspect ratios (AR) of square cavities were used.	Effect of Aspect Ratio.	Numerical	When the AR is increased, the total melting time takes longer, valid for both the left and bottom wall heating circumstances.

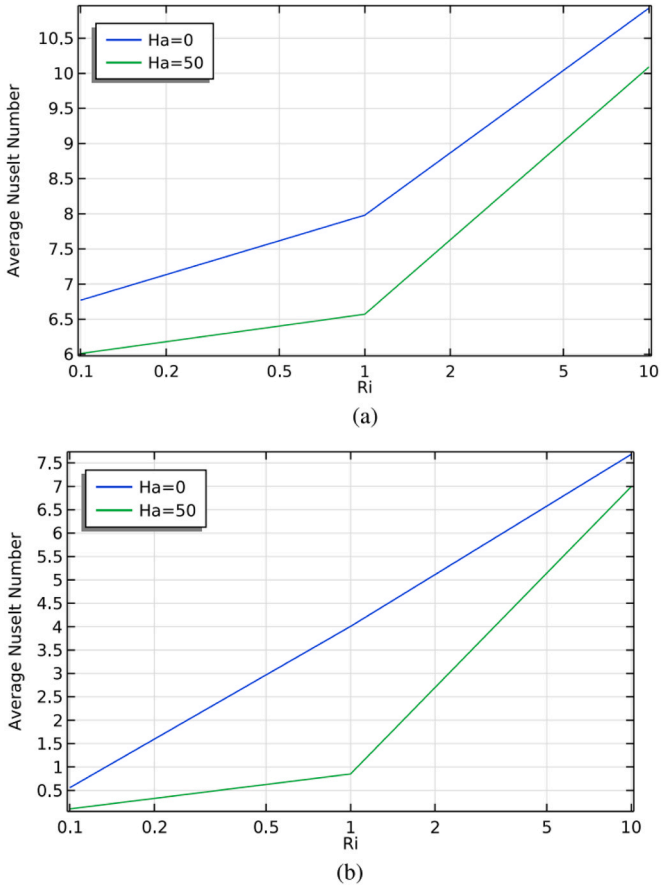

Fig. 13. Average Nusselt number variation along the bottom (a) and top wall (b) with Ri forHa = 0, 50 (Ibrahim and Hirpho, 2021).

significantly affected by the cavity angle, although to a lesser extent by the tube size.

In a partly heated trapezoidal chamber filled with non-Newtonian Casson fluid, Hamid et al. (2019) described the process of natural convection flow. The governing flow equations were derived using a

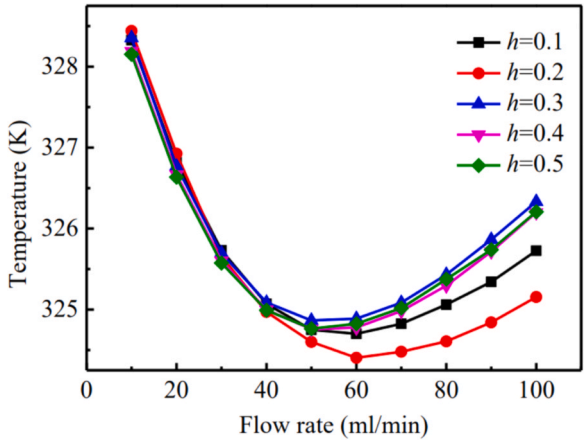

Fig. 14. MHX hot water outlet temps vary with ITRC height (Pan et al., 2018).

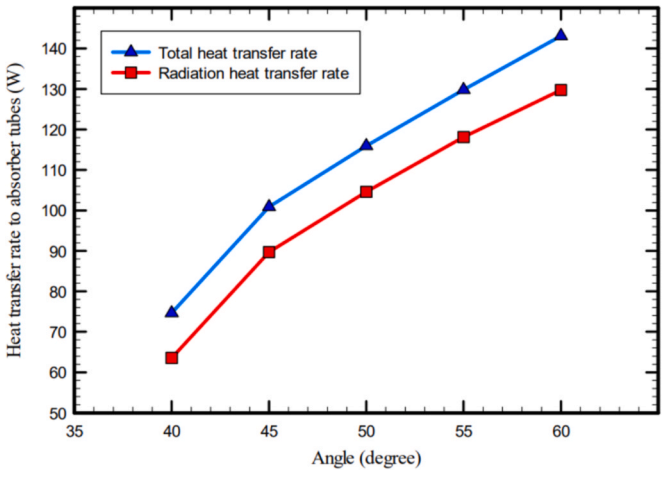

Fig. 15. Total and radiation heat transfer from the cavity to the absorber tubes in models with varied cavity angles (Dabiri et al., 2018).

non-Newtonian model of Casson fluid. The lower wall of the cage was partly heated and used to regulate the temperature within. The Galerkin finite element method (GFEM) investigated the dimensionless PDEs system's solution. Isotherms and streamlines were used to visualise the flow and temperature fields, respectively, while the simulations for the flow and temperature fields were run across a range of Rayleigh numbers ($10^4 \leq Ra \leq 10^5$) and lengths of the heated component. It was shown that the x- and y-axis velocities become more prominent when the Casson fluid parameter is reduced. At the cavity's centre, the Nusselt number is most affected by changes in the Casson fluid parameter, whereas the number rises with the length of the heated bottom wall.

A restricted slot jet impinging into an open trapezoidal cavity with a porous layer was studied by Hussain et al. (2020). A thin, porous layer covers the cavity and was exposed to a cold impingement air jet, which helps make the research relevant to a real-world situation. The porous layer followed the Darcy-Forchheimer model, and its porosity was chosen to maintain a constant temperature difference between the fluid and the porous matrix. To arrive at a numerical solution, the finite element approach was used. The results revealed that the porous layer thickness should be kept to a minimum; raising it from 0.1 to 0.3 decreases the average Nusselt number by 17% when the Darcy number is 10^{-3}, as shown in Fig. 16. It was also discovered that the trapezoidal cavity aids in rapidly maturing to an adult state.

To evaluate the effectiveness of a design innovation for a rectangular microchannel heat sink, Datta et al. (2019) offered a numerical inquiry that applies the ideas of maximization of thermal performance (TP) and minimisation of entropy production (EG). The channel was envisioned as a series of modifying units, each with a rib centered between two trapezoidal cavities (TRC) on opposing wall surfaces. A three-dimensional laminar-flow conjugate heat-transfer analysis was performed between Reynolds numbers (Re) of 140 and 600 using the SIMPLEC algorithm for the flow and conduction through the boundary walls and the interior ribs. The bulk fluid temperature rise was minimal, and the substrate temperature increase was much lower due to copper's significantly better thermal conductivity than silicon. The rectangular (RR), reverse triangular (BTR), forward triangular (FTR), and diamond (DR) rib configurations have all been examined. Copper and silicon have emerged as having equivalent expected variations of all performances, with copper delivering the greatest TP of roughly 2.31 compared to 1.96 observed with silicon.

A computational investigation was conducted by Gowda et al. (2019) to investigate a trapezoidal cavity created by an inclined left heated wall

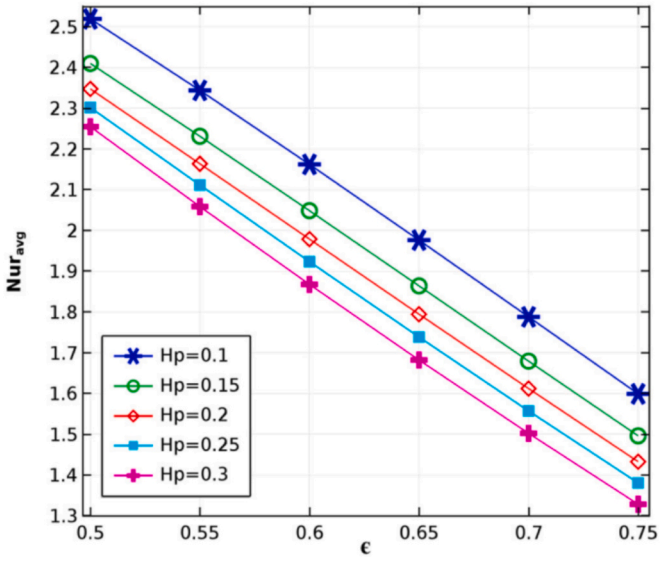

Fig. 16. Normalized Nusselt Number variation with ϵ and Hp for$Re = 500$ and$Da = 10^{-3}$ (Hussain et al., 2020).

and insulated bottom horizontal walls using a control volume approach. The calculations were conducted for a range of Ra from 10^3 to 10^7, with the heated wall being oriented at angles of $\phi = 60$ and 120. The study compared the outcomes of scenarios where the vertical wall remains closed and scenarios where the vertical wall has various openings. The comparison was based on the variations observed in isotherms, stream functions, local thermal rates, and mean heat transfer rates. The Nu exhibited a positive correlation with the Ra, indicating that an increase in the Ra led to a rise in the Nu. Conversely, there was a negative relationship between the Nu and the angle of direction, suggesting that an increase in the angle of direction resulted in a reduction in the Nu. The transition area from conduction to convection occurred at approximately a Ra of 5×10^3. The case that possesses vents at the extreme ends has been found to demonstrate the highest level of heat transfer compared to other cases. The heat transfer is more efficient when the orientation angle is 60 degrees. Compared to a uniformly cooled wall, the heat transfer increases by 24%, 40%, 57% and 75% at Ra of 10^4 - 10^7, respectively.

The flow and heat transmission in a trapezoidal cavity were studied statistically by Khan et al. (2020). The experiment used a porous media with a low Darcy number and a water-based ferrofluid containing Fe_3O_4 nanoparticles. The top wall was adiabatic, the bottom wall was heated, and the sides were kept at a constant cold temperature. The finite element approach was used to solve the governing equations, which are dimensionless statistically. The whole area was subjected to a B0 homogeneous magnetic field. The induced magnetic field is believed to be negligible since the magnetic Re is substantially less than the applied magnetic field. The walls were not given any slip boundary constraints. Dimensionless velocity and temperature within the cavity were used to construct streamlines and isotherms. It was shown that the magnetic field, thermal buoyancy, permeability of the porous media, and the size of the heating element all play essential roles in increasing the dimensionless mean thermal transport rate.

Iachachene et al. (2019) conducted a transient two-dimensional numerical investigation of melting a PCM in a trapezoidal cavity using the enthalpy-porosity method. To examine how PCM performance varies depending on orientation, paraffin wax was first used to fill the hollow. The nanofluid thermal performance was then compared to that before and after adding graphene nanoparticles to the pure PCM to ascertain whether or not the latter could counteract the former's enhanced orientation effect. In place of using simple mixture models or correlations, they selected to utilise experimental data for the latent heat of fusion and the thermal conductivity of solid NePCM. Melt fraction as a function of melting time was shown with temporal velocity and temperature graphs. Both effects were advantageous in improving heat transport in PCMs, as demonstrated by the simulation results. When the improvement in nanofluid thermal conductivity was less than 80%, NePCM resulted in worse heat transfer performance.

The laminar flow of a nano liquid in a trapezoidal cavity was studied numerically by Mebarek-Oudina et al. (2021), and convective exchanges were measured. The cavity in issue is a right-angle trapezium, and it holds a hybrid Cu-Al_2O_3/Water nanofluid mixture. An external magnetic field acted uniformly at an inclination angle γ of on the enclosure with the zigzag wall. The permeable domain has been modelled using Darcy-Forchheimer. Different Hartmann numbers ($0 \leq Ha \leq 100$), rotational velocities ($-4000 \leq \omega \leq 4000$), magnetic field inclination angles ($0° \leq \gamma \leq 90°$), Rayleigh numbers ($10^3 \leq Ra \leq 10^5$), cylinder radii ($5 \times 10^{-2} \leq r \leq 0.2$), different volumetric fractions ($0 \leq \phi \leq 0.08$), and so on were all tested for their effects. The outcome indicated that a magnetic field has a meaningful impact on the nanofluid's flow and that increasing the cavity's Ra and Hartmann numbers improved its thermal performance.

Within a trapezoidal enclosure with a specific heat and mass source at the bottom wall of the cavity, Mondal and Mahapatra (2021) explored numerically double-diffusive, Magnetohydrodynamics (MHD), mixed convection flow of Al_2O_3-water nanofluid. Entropy creation from fluid

friction was explored alongside related phenomena such as heat, mass transport, and magnetic fields. This analysis considered a wide range of inclination degrees and aspect ratios. The governing equations were solved using the biconjugate gradient stabilized technique (BiCGStab) using finite difference approximations of the second and fourth orders. It has been shown that the Richardson number (Ri=0.01) significantly impacts the entropy production rate, with smaller values resulting in less entropy production. To minimise entropy generation, the research found that a rectangular cavity with a low magnetic field and aspect ratio is ideal and that a heat and mass source in the cavity's middle lower wall is generally well-received.

The thermal performance of a nanofluid within a trapezoidal chamber with an elliptical barrier was given by Shah et al. (2021). The slanted walls were insulated (adiabatic) and kept inside at a constant (cold) temperature. The cavity's top horizontal wall is a conductor for the energy that propels the always-moving, split lids. The finite element technique solved the dimensionless system of velocity, temperature, and concentration partial differential equations. When graphically interpreted, these profiles showed that the Lewis number significantly affects the isotherms and concentrations. Maximum heat transmission was attained along the inner direction of the lid walls for lower values of the buoyancy ratio parameter. Due to the significant thermal diffusion over the whole domain of the cavity, the Lewis number has been shown to have a considerable influence on isotherm and concentration.

Natural convection in a porous trapezoidal cavity was analysed by Khan et al. (2021) using a non-equilibrium thermal energy transfer model. The thermal behaviour was studied by inserting barriers into the cavity and heating either the bottom wall or the whole model. However, the steady-state condition was used to get numerical results even though the governing energy and momentum equations are unstable. Mathematical modelling of the physical issue and subsequent numerical simulation through the finite difference technique was presented. It was shown that the isotherms and streamlines are dispersed symmetrically around the obstacles and that thermal non-equilibrium is affected by the parameters and H. For both fluids and solids, the Rayleigh and the local Nusselt numbers showed a dominating improvement, but the average Nusselt number decreased with an increase in the heating domains.

Using the lattice Boltzmann technique, Ebrahimi et al. (2023) investigated the mixed convection of a nanofluid within an oblique trapezoidal cavity subject to a multi-directional magnetic field. The moveable top wall of the trapezoidal-shaped hollow was kept cold, while the bottom wall was heated sinusoidally. All the characteristics associated with the flow and temperature fields were calculated in the simulations using the temperature and flow distribution functions. Results showed that a higher Rayleigh number and lower Richardson number resulted in more efficient heat transmission. Similarly, increasing the nanoparticle volume percentage while holding all other factors constant resulted in a larger mean Nusselt number. Heat transmission was diminished when the Hartmann number rose because flow velocity inside the hollow was slowed. Changing the magnetic field angle and the cavity's slope may modify the flow and heat transmission. The effect of a magnetic field on heat conduction was enhanced when applied. In the cases of Ri= 0.1, 1, and 10, the Nu_{avg} decreases from 20 to 5 (a reduction of 4%) when the Hartmann number rises from 0 to 100.

Fluid flow and buoyant heat transfer in a porous trapezoidal cavity were discussed by Kumara et al. (2023), who demonstrated the effect of aspect ratio and different temperature boundary conditions. A homogeneous, linear, and non-uniform temperature gradient was applied to the base wall, while the higher and steep walls were kept at a constant cold temperature. The Darcy model was used in this research. The governing equations were solved using the finite element method with the help of a simple algorithm. The findings demonstrated that the heat transmission rate increases for fixed aspect ratios as the Rayleigh number rises. The rate of heat transmission reduced as the aspect ratio increased. The results were presented in the forms of local and mean Nusselt numbers, functions of the stream, and isotherm functions.

The mixed convection of a NePCM within a trapezoidal-wavy cavity with an applied magnetic field was studied by Qasem et al. (2023). The cavity's top lid moves in and out, and the temperature differential between the slanted, chilly side walls and the hot bottom wavy wall causes mixed convection. Galerkin finite element technique (GFEM) was used to find solutions to the governing equations that characterised the scenario under study. Analysis of the thermal behaviour and flow patterns was performed for a range of lid velocities Re = 1–1000), bottom wall undulation numbers (N = 1–4), and magnetic field strengths (Hartmann number (Ha) = 0–100). Based on the data, the authors realised that the mean Nu is related to the lid velocity (Re) but inversely related to the number of bottom wavy undulations (N) and the magnetic field intensity (Ha). Local Nu values may be multiplied by a factor of 300 for larger Re (e.g.,Re = 1000) compared to smaller values of Re (e.g.,Re = 1). AtRe = 1000, the mean Nu was decreased by 54% and 31%, respectively, when Ha was increased from 0 to 100, and N was increased from 1 to 4. Table 3 presents a summary of the associated studies outlined on the trapezoidal cavity.

2.4. Review of triangular cavity

Multiple engineering branches benefit significantly from applying natural convection practices in cavities of varying shapes and sizes filled with fluid. This includes power engine stations, materials processing, thermal insulations, climate control, electronic systems, automotive engineering, fire extinguishing systems, etc. The creation of a temperature difference between regions causes convective heat transfer to occur in constrained geometries. Fluids with unique properties, called heat-transferring liquids, accomplish energy processes in enclosed geometries. Research on the triangular hollow is detailed below.

The effect of a rectangular heat source in a confined area on natural convection flow via a triangle cavity was established by Fayz-Al-Asad et al. (2021). Using a Galerkin weighted residual process inside a finite element framework, the current issue was described as non-linear governing equations. The impact of the Rayleigh number (Ra) on the flow pattern and temperature change inside an enclosure was studied over a range of Ra values at a pressure ratio (Pr) of 0.71. Graphs showing streamlines, velocity profiles, isotherms, rectangular bar efficiency, mean Nusselt number and average fluid temperature provided the numerical answers to the question. The obtained results confirmed that the rate of heat fluctuation inside a triangular cavity increases as the Rayleigh number increases. Fig. 17 shows that given a specific size of the rectangular heat source, the global Nusselt number improves gradually with increasing Ra. In addition, we found that when the dimensions of the rectangular heat source were raised, the mean Nusselt number decreased.

A numerical study of thermal convection within a lid-driven triangular cavity was published by Soomro et al. (2020). Based on magneto-hydrodynamics (MHD), a continuous magnetic field of strength B0 was applied along the horizontal x-axis. The slanted sides were adiabatically smooth because of how the chamber was shaped. Convection heat transfer occurs because the cavity's top wall moves, and its surfaces have different temperatures. Nonlinear partial differential equations with boundary conditions influence flow and heat transport phenomena. To find a numerical answer, the finite element method was used. Emerging physical parameters, such as Reynolds number ($200 \leq Re \leq 600$), Richardson number ($0.01 \leq Ri \leq 1.0$), and Hartmann number ($0 \leq Ha \leq 20$), were used in the simulation. A higher Richardson number was shown to enhance the heat transfer rate, whereas a higher Hartmann number had the opposite effect.

Considering radiation effects and an inclined constant magnetic field (MF), Afrand et al. (2020) investigated the free convective heat transfer and entropy formation of an alumina/water nanofluid in a slanted triangle enclosure. The governing equations were solved using the SIMPLE technique. Convective heat transfer, entropy generation, and the Bejan number (Be) were analysed to determine the influence of influential

Table 3
Studies outline on trapezoidal cavity.

Authors (year)	Structure	Examined variables	Study method	Results / Impacts
Ibrahim and Hirpho (2021)	Cavity-shaped isosceles trapezium.	The influence of the amplitude of the temperature oscillation and the strength of the magnetic field.	Numerical	Whenever there is an increase in the amplitude of the temperature oscillation function, the Nusselt number experiences an upward trend. In addition, when the magnetic field's strength increases, the Nusselt number's average value decreases.
Alfellag et al. (2019)	A microchannel heat sink (MCHS) with plate fins, trapezoidal cavities, and oval pins with and without slots.	The three parameters of interest are the aspect ratio of the oval pins, the pin location relative to the cavity center towards the inlet, and the thickness of the two sloping slots of the pins.	Numerical	The suggested design's best configuration calls for a pin aspect ratio of (AR = 1.3), pin distance from the cavity center of (x = 0.03 mm), and slot thickness of (t = 0.008 mm). This combination results in a maximum PEC of 1.37.
Pan et al. (2018)	A plate microchannel heat exchanger (MHX) that has isosceles trapezoid-shaped reentrant cavities (ITRCs) in the sidewalls. MHX stands for microchannel heat exchanger.	The influences of the structural parameters of the ITRCs.	Experimental and Numerical	The rise in the coincidence degree of the ITRCs leads to reduced heat transmission performance. Compared to the performance of the from-sparse-to-dense (FSTD) ITRC distribution, which is better at bigger flow rates, the heat transfer performance of the from-dense-to-sparse (FDTS) ITRC distribution demonstrates benefits at flow rates lower than 60 ml/min.
Nayak et al. (2018)	Trapezoidal shaped solar cooker.	Mode of losses.	Experimental and Numerical	Radiation may account for the vast majority of heat loss, but natural convection contributes 20–30%, making it a significant contributor.
Dabiri et al. (2018)	The Fresnel reflector of the linear type has a trapezoidal cavity.	The effects of the cavity angle and the impact of the tube size.	Experimental and Numerical	The overall value for heat transfer rate is raised when the cavity angle is increased; however, the heat received by each tube is reduced when this is done. According to the findings, the cavity angle has a far more significant impact on the heat transmission rate than the tube size.
Hamid et al. (2019)	Chamber in the shape of a trapezium that is only partially heated and contains a non-Newtonian Casson fluid.	Casson fluid parameter and.	Numerical	The velocities in the x-direction and the y-direction show the prevailing behavior when the Casson fluid parameter drops. While the impact of lower values of the Casson fluid parameter on the Nusselt number is considerable at the cavity's center, the Nusselt number continues to rise as the length of the cavity's heated bottom wall grows.
Hussain et al. (2020)	A confined slot jet will impact an open trapezoidal cavity with a porous layer.	Effect of thickness of the porous layer.	Numerical	When the Darcy number is 10, increasing the thickness of the porous layer from 0.1 to 0.3 results in a 17% decrease in the average Nusselt number. The optimal thickness of the porous layer should be as minimal as feasible.
Datta et al. (2019)	A rib is positioned symmetrically between two trapezoidal cavities (TRC) on opposing side walls.	Impact of using copper and silicon ribs.	Numerical	Copper has a TP of around 2.31, much higher than the 1.96 in silicon.
Gowda et al. (2019)	Heated inclined walls on the left and insulated horizontal walls on the bottom made a trapezoidal hollow.	Effect of orientation angle and Ra.	Numerical	An orientation angle of sixty degrees produces the best results for heat transmission. Compared to a wall that is evenly cooled, the heat transmission rate increases by 24%, 40%, 57%, and 75%, respectively, when Ra equals 10^4, 10^5, 10^6, and 10^7.
Khan et al. (2020)	A trapezoidal cavity filled with a ferrofluid based on water contains nanoparticles of Fe3O4 and a porous medium with a low Darcy number.	The length of the heat source, the porosity of the porous media, thermal buoyancy, and the magnetic field.	Numerical	Several factors, including the magnetic field, thermal buoyancy, the permeability of the porous media, and the length of the heating element, greatly influence the increase of the dimensionless average heat transfer rate.
Iachachene et al. (2019)	PCM embedded in a trapezoidal cavity.	Effect of NePCM.	Numerical	NePCM led to a lower heat transfer performance when the nanofluid thermal conductivity enhancement was less than 80%.
Mebarek-Oudina et al. (2021)	The cavity is geometrically trapezoidal at right angles containing a hybrid Cu-Al_2O_3/Water nanofluid.	Effect of a magnetic field, Ra, and Hartmann numbers.	Numerical	The introduction of a magnetic field significantly impacts the flow of the nanofluid, and the enhancement of the Ra and Hartmann numbers leads to an improvement in the thermal performance of the cavity.

(*continued on next page*)

Table 3 (*continued*)

Authors (year)	Structure	Examined variables	Study method	Results / Impacts
Mondal and Mahapatra (2021)	Within a trapezoidal enclosure with a distinct source of heat and mass at the bottom wall of the hollow, a mixed convection flow of Al_2O_3-water nanofluid is seen to be moving.	Richardson number.	Numerical	To a large extent, entropy formation is determined by heat transfer, and having lower values of the Richardson number (Ri=0.01) brings a reduction in that phenomenon.
Shah et al. (2021)	A nanofluid is contained inside a trapezoidal chamber with a split lid and is propelled by an elliptic-shaped barrier.	The impact of emerging parameters such as Richardson number ($10^{-2} \leq Ri \leq 10$), Lewis number ($0.1 \leq Le \leq 10$), Reynolds number ($300 \leq Re \leq 500$) and buoyancy ratio ($-10 \leq Br \leq 10$).	Numerical	While the buoyancy ratio parameter has a lower value, the highest heat transmission is achieved while looking toward the lid walls. Because of the high level of heat diffusion over the cavity, the Lewis number demonstrates that the primary influence at isotherm and concentration is the latter.
Khan et al. (2021)	Natural convection inside a porous trapezoidal cavity while a non-equilibrium thermal energy transfer model is considered.	Effect of Local and Average Nusselt Numbers	Numerical	The local Nusselt and average Nusselt numbers exhibit a dominating augmentation for both fluids and solid phases, supported by Rayleigh numbers while decreasing with an increase in the heating domains.
Ebrahimi et al. (2023)	An inclined trapezoidal cavity was found in a magnetic field that runs in several directions.	The impacts of varying Rayleigh numbers and Richardson numbers, inclined cavity angles, volume percentages of nanoparticles, magnetic field strength, and applied magnetic field angle were investigated.	Numerical	Increases in the Rayleigh number and decreases in the Richardson number lead to heat transfer improvements. Increasing the volume percentage of nanoparticles will increase the average Nusselt number. This may be thought of as a corollary. When the Hartmann number is raised, the flow speed inside the hollow decreases, reducing the amount of heat transferred. Changing the slope of the cavity's slope and the angle at which the magnetic field is directed has an impact on the flow and heat transfer. In the cases when Ri= 0.1, 1, and 10, the Nu_{avg} value goes from 20 to 5 (a decrease of 4%), while the Hartmann number goes from 0 to 100.
Kumara et al. (2023)	A trapezoidal void that is permeable.	The influence of the aspect ratio and the many different temperature boundary conditions.	Numerical	The heat transmission rate rises with increasing values of the Rayleigh number, provided that the aspect ratio remains the same. The heat transmission rate slows down when there is an increase in the aspect ratio.
Qasem et al. (2023)	A magnetic field is applied to NePCM inside a cavity with trapezoidal-wavy walls.	The influence of the magnetic field as well as the wavering of the wall.	Experimental and Numerical	The average Nusselt number is inversely related to the bottom wavy undulation number (N) and the magnetic field intensity (Ha), but it is directly proportional to the lid velocity (Re). Compared to the lower Re values, the higher Re values have the potential to bring about a 300% increase in the importance of the local nu. At a Re value of 1000, the mean Nusselt number of 53% and 30% was reduced by raising Ha from 0 to 100 and N from 1 to 4.

factors, including Ra, Ha, MF angle, enclosure angle, radiation parameter, and concentration of alumina nanomaterials. The results showed that when Ra is raised, the heat transfer rate (HTR) and the entropy generation rise by 2.32 and 14.17, respectively. Increasing the Ha reduces the HTR and total entropy production (TEG). To improve, the Be reduces the Ra and increases the Ha. The HTR is at its highest at an MF angle of 90° and an enclosure angle of 60°. When added to water at a concentration of 6%, the nanomaterials improved both the HTR and the TEG by 7.3% and 9.3%, respectively.

Using a partly heated triangular chamber with a heated cylinder impediment, Haq et al. (2019) studied the thermal management of water-based single-wall carbon nanotubes (SWCNTs). The SWCNT was added at the inner circular cylinder of this model to increase the thermal conductivity of the liquid and the model as a whole. The surface of the heat cylinder was specified in three different circumstances (cold, heated, and adiabatic) to maintain thermal management. The temperature gradient between the cavity's excellent slanted sides and the bottom wall, which is only partially heated, causes convection. Finite Element Method (FEM) was used to get a numerical answer. According to the results, the heat transfer rate for the hot cylinder was lower than that of the cold cylinder at the heated length. However, it rises when the Rayleigh number and the proportion of nanoparticles in a given sample grow. In addition, a higher volume proportion of nanoparticles improved temperature dispersion within the cavity. Increases in magnetic field effects, on the other hand, have little to no influence on the temperature gradient.

Microchannels with triangular cavities and rectangular fins (Tri.C-Rec.F) were created by Li et al. (2020) to enhance flow boiling. Pure acetone was used in the trials, and the input temperature was constant at 29 °C. The mass fluxes tested were 83 kg/(m^2 s), 147 kg/(m^2 s), 324 kg/(m^2 s), and 442 kg/(m^2 s), while the effective heat flux varied from 0 to 101 W/cm^2. Tri.C-Rec.F microchannel flow boiling properties were investigated and compared to those of a standard rectangular microchannel (R). Microstructures' ability to disrupt the flow and micro fins' ability to break up bubbles facilitated bubble departure and reduced flow reversal. The highest increase in heat transfer coefficient for microchannel Tri.C-Rec.F over microchannel R was 300% at G= 83% and 51.6% at 442 kg/(m^2 s), as shown in Fig. 18. Increased pressure loss was caused by the micro fins' acceleration, disturbance, and separation effects; this design flaw is amenable to optimisation.

The effects of Brownian diffusion and thermophoresis on a water-based nanofluid's free convection within two entrapped triangular

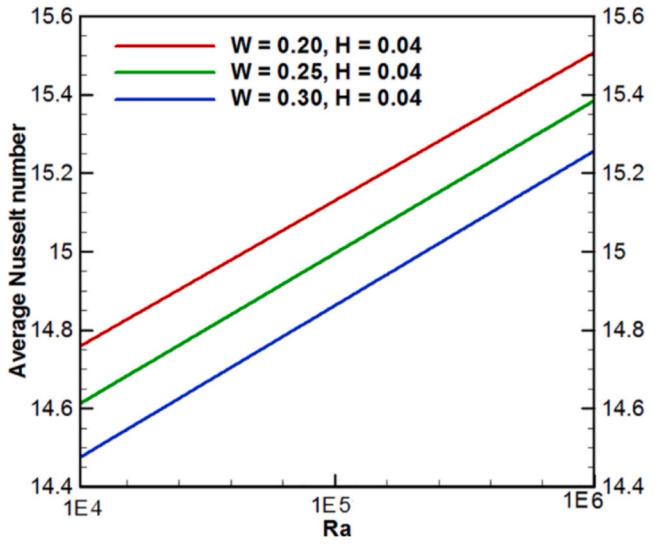

Fig. 17. Nu_{avg} for various values of W and Ra at with = 0.71 (Fayz-Al-Asad et al., 2021).

cavities were explored numerically by Sheremet et al. (2017). Constantly high temperatures were maintained along the bottom and top walls of the cavities, while the other walls were preserved at low temperatures. The second-order accuracy finite difference approach was used to solve the dimensionally free governing equations that were developed using the stream function, the vorticity, the temperature, and the concentration of the nanoparticles. Fluid flow, heat transmission, and mass transfer have all been studied concerning the Rayleigh number, the Lewis number, and the buoyancy-ratio parameter. Under the assumed temperature boundary conditions, it was discovered that the lower triangular cavity is more susceptible to changes in the Rayleigh number and buoyancy ratio parameter than the upper cavity. The Rayleigh number and the buoyancy-ratio parameter rise when nanoparticles are distributed unevenly inside a cavity.

Gangawane et al. (2019) studied the effect of relocating a triangular block subject to a constant heat flux (CHF) thermal condition on the two-dimensional steady laminar mixed convective fluid circulation and heat transfer in a square lid-driven cavity. Various experiments have been conducted to determine the impact of shifting the block's position along the cavity's vertical axis (x = 0.5, y = 0.5). Different dimensionless parameters that govern the flow have been illustrated, including the Reynolds number Re = 11000), the Richardson number (Ri =0.01, 1, 10), the blockage (B =0.1, 0.2, 0.3), and the location (Ly =0.25, 0.5, 0.75). Compared to the other two positions tested (Ly = 0.25, Ly = 0.75), the centered block location (Ly=0.5) was shown to have the highest heat transmission rates. Nusselt number decreases for a fixed obstruction as a function of rising Ri.

Thermo-physical properties of viscous material in a triangle enclosure interacting with a heated square cylinder in the center were studied by Bilal et al. (2020). Laminar, stable, incompressible viscous material was studied for two alternative thermal conditions in which the bottom wall is either (a) uniformly heated or (b) non-uniformly heated to see thermal features explicitly. Dimensional partial differential expressions were used to mathematically model phenomena. Compared to a uniformly heated wall, heat from a non-uniformly heated base wall was more efficient and effective. In this regard, it is important to note that a singularity arises in the case of a constant heat supply but disappears in the case of a non-uniform heat supply. Fig. 19 shows encouraging tendencies in the Nu and kinetic energy as the Ra increases. It is also discovered that the average velocity magnitude over the whole cavity grows for growing values of the Ra.

Nanofluid conjugate natural convection heat transport was studied by Zadeh et al. (2020) in a square cage with two solid triangular sides. T_h and T_c were maintained on the cavity's left and right walls, while the bottom and top were kept at ambient temperatures. Due to thermophoresis and Brownian motion, the Buongiorno model was used to evaluate the nanoparticle distribution within the cavity. Galerkin finite element technique was used to solve the governing nonlinear equations on a non-uniform unstructured grid. Isotherm, streamlined headline, and concentration contours, as well as local and mean Nu values, were presented from the numerical data. Incorporating the triangular blocks increased the total rate of heat transmission, as shown by the experimental data. As the thermal conductivity ratio (R_k) becomes lower, average Nusselt numbers increase. When the triangle walls are inverted, heat transmission slows down considerably.

Yao et al. (2021) presented a novel construction of a microchannel with a triangular chamber and rib to improve heat transmission. Multi-objective optimisation using Response Surface Methodology (RSM), Non-dominated Sorting Genetic Algorithm (NSGA-II), and

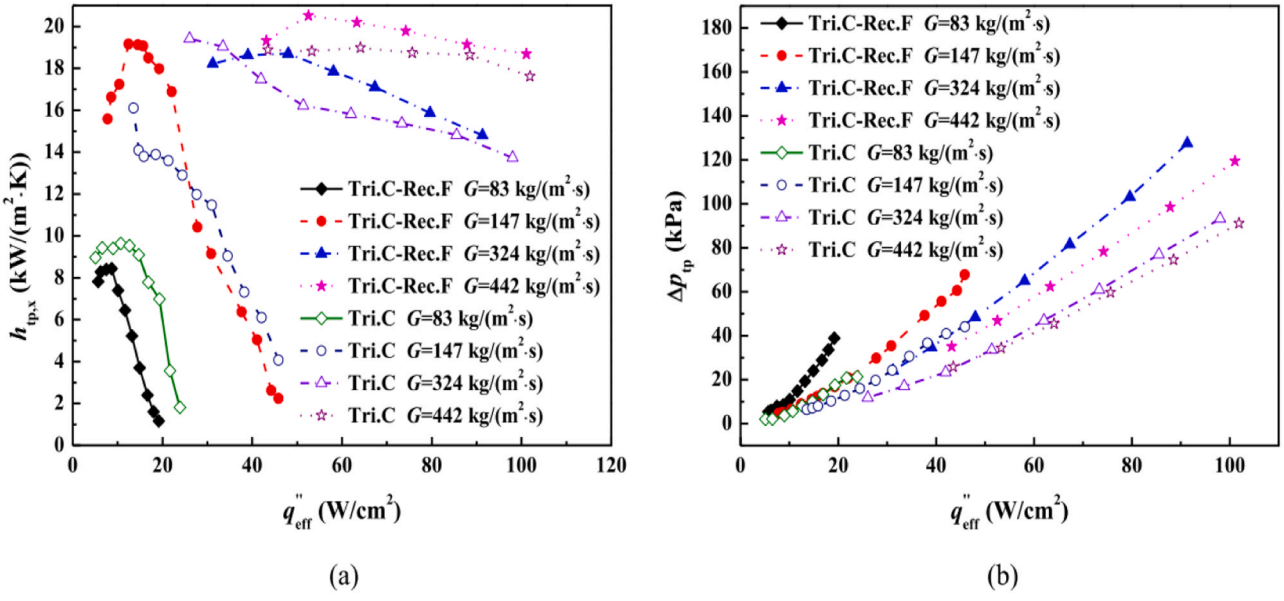

Fig. 18. (a) Two-phase heat transfer coefficient and (b) pressure drop (Li et al., 2020).

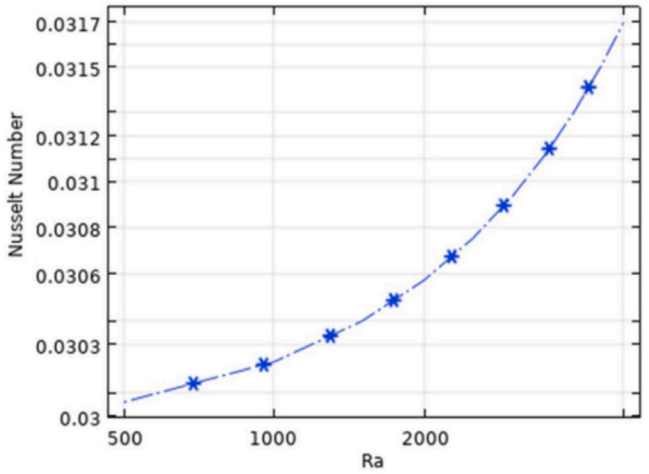

Fig. 19. Nusselt vs Rayleigh number (Ra) (Bilal et al., 2020).

k-means clustering to determine a Pareto front yielded good thermal performance. Objective functions (thermal resistance (R_{th}) and pumping power (PP)) were optimised by varying design factors (cavity height, rib height, and Reynold number) over 30 numerical data sets. Convective heat transfer was much larger than heat conduction and heat loss in the total quantity of heat transferred throughout the process. The Pareto front was split into five sections using k-means clustering, with the optimal heat transmission characteristics occurring at intermediate values of R_{th} and PP. The temperature gradient between the fluid and the heating wall was reduced from 26 K to 17 K after optimisation of the rectangular microchannel. Case 4 (e1 = 0.0572 mm, e2 = 0.0224 mm) showed the highest thermal performance for a thermal enhancement factor of 1.2305, thanks to the complementary effects of the flow rate and temperature gradient.

In a numerical study of natural convection in a cavity, Wijayanta (2021) found a solution to the thermal analysis problem. The authors proposed simulating laminar natural convective heat transport in triangular cavities using the direct meshless local Petrov-Galerkin technique in conjunction with an implied reproduction model. Using the Dirac function as a test function, the spatial components of the governing equation were discretized through the direct meshless local Petrov-Galerkin technique. Using a reproduction methodology, the approach directly coupled the pressure with the velocity components. A perfect agreement was found between numerical results produced using the suggested technique and those obtained using the standard methods accessible in the literature. Two movement cells were observed for small Prandtl numbers ($0.026 \leq Pr \leq 0.7$): primary movement cells in the cavity's sweet spot and secondary circulation cells in the four corners. For large Prandtl numbers ($0.7 \leq Pr \leq 1000$), the secondary circulation disappears altogether because it is much weaker than the central circulation.

Mixed convective heat transport was modelled by Shahid et al. (2021) in a right triangular hollow with a heated cover. There was regular incompressible fluid within the cavity. Using the multi-relaxation time collision model, researchers examined heat transfer and fluid flow using the D2Q5 and D9 models of the lattice Boltzmann technique. The effects of the Richardson number (Ri=0.01–100), the Grashof number ($10^4 \leq Gr \leq 10^7$), and the Prandtl number Pr = 0.71, 1 and 7) on fluid behaviour and heat transport were investigated. They emphasised the directional movement of the revolving lid. The buoyant forces were shown to rise with increasing Gr. This means that natural convection will significantly impact more than induced convection. The overall Nusselt number is higher now than it was before.

Using the finite volume approach, Shekaramiz et al. (2021) performed a numerical investigation of Buongiorno's model for calculating the volume fraction of iron oxide nanoparticles within a triangular chamber with a heated wavy wall. Entropy formation and the heat transmission rate may be increased by using a uniform magnetic field. One side of the chamber was held at a constant temperature while the other was subjected to a periodic temperature boundary condition. The inclination angle, undulation number (n), and Hartmann and Rayleigh numbers (Ha and Ra, respectively) of magnetic field changes were studied. The findings indicated that the number of undulations significantly impacts the heat transmission rate. Nusselt number is closely connected to Ra and is inverse to the undulation number. The heat transfer rate also correlates negatively with the entropy production rate.

Xiong et al. (2021) conducted numerical simulations to analyse the mixed convection flow of a Newtonian fluid in a lid-driven triangular cavity with adiabatic circular obstacles on the left and right sides. The flow characteristics and heat transfer phenomena were investigated using nonlinear partial differential equations (PDEs). The effects of various physical parameters, such as Reynolds number, Hartmann number, Richardson number, and local Nusselt number, on the velocity and temperature distributions were examined. The findings indicated that an increase in the Hartmann number leads to a reduction in the rate of heat transfer, whereas the Richardson number showed the opposite behaviour. The Richardson number was shown to contract the velocity contours and the thickness of the flow boundary layer. Furthermore, it was observed that buoyant motion and heat transfer rates increase with higher shear rates for larger Richardson numbers. Higher Reynolds numbers resulted in expanded velocity profiles, creating significant cavities on the side of the obstacles. Moreover, the Reynolds number was positively correlated with the heat transfer rate, and the Hartmann number has a significant influence on fluid flow resistance due to its strong magnetic field.

Laminar flow and thermal convection of H_2O/SWCNT nanofluid were simulated by Sarlak et al. (2023) using the finite volume approach in a triangular cavity. There was a warm source at the bottom of the triangular cavity, and the low temperature of the cavity was caused by the forced flow of low-temperature H_2O flowing above the hollow. The range of parameters considered in this analysis was between $\varphi = 0$–0.06, with the angle of attack between 15° and 60° and the Rayleigh number set at 10. It has been determined that the temperature difference between the low and high-temperature sources in the cavity significantly impacts its temperature differences. As the angle of attack increases, so do the temperature differences within the cavity. Heat transmission may be enhanced by injecting fluid into the cavity and increasing the loading of the nanoparticles (φ). The momentum dissipation rate of the cooling fluid increases as its viscosity and density increase with increasing. Table 4 presents a summary of the conducted studies outlining triangular cavities.

3. Critical evaluation of heat transfer in various cavity geometries based NePCMs and nominal improvements

The use of Nano-Enhanced Phase Change Materials (NEPCMs) for TES and control has shown significant potential. The container geometry that NEPCMs are housed in can have significant effects on their thermal characteristics, more especially, on their overall thermal conductivity. The use of containers with four various cavity shapes (spheres, squares, trapezoids, and triangles) is examined in this thorough analysis, and it is determined whether they have an impact on enhancing the thermal properties of NEPCMs.

- Spherical containers offer a quick and effective approach to contain NEPCMs. Their curved surfaces minimize temperature differences inside the material and aid in effective heat distribution. Spherical containers can be less space-efficient when stacked, which restricts their use in systems with limited space. Additionally, it may be difficult to achieve uniform dispersion of nanoparticles within the spherical PCM, which could have an impact on the overall

Table 4
Studies outline on triangular cavity.

Authors (year)	Structure	Examined variables	Study method	Results / Impacts
Fayz-Al-Asad et al. (2021)	Natural convective flow-through triangular cavity.	Width of the close space rectangular bar and Ra.	Numerical	An increase in Ra leads to a steady and consistent improvement in the global Nusselt number for a given size of the rectangular heat source.
Soomro et al. (2020)	Convection heat transfer inside the lid-driven triangular cavity.	Richardson number and Hartmann number.	Numerical	A rise in the Richardson number increases the heat transfer rate, while an increase in Hartmann has the opposite effect.
Afrand et al. (2020)	Nanofluid alumina/water contained inside an inclined triangular enclosure with consideration given to the effects of radiation and an inclined magnetic field (MF).	The influence of effective parameters includes Ra, Ha, the magnetic field angle, the enclosure angle, the radiation parameter, and the concentration of alumina nanomaterials.	Numerical	When the Ra was raised, there was a corresponding rise of 2.32 times in the heat transfer rate (HTR) and a 14.17 times increase in the entropy generation. The Be improves the situation by lowering the Ra and increasing the Ha. When 6% of the nanomaterials were introduced to the water, there was a 7.3% increase in the HTR and a 9.3% increase in the TEG.
Haq et al. (2019)	Single-walled carbon nanotubes (SWCNTs) are water-based and placed within a partly heated triangle-shaped chamber containing a heated cylindrical barrier.	The impacts of cold, adiabatic, and hot cylindrical barriers, heated lengths, the Ra, the nanoparticle loading, and the magnetic parameter.	Numerical	When measured along the heated length, the heat transmission rate from a hot cylinder is lower than that of a cool cylinder. On the other hand, it rises due to an increase in the nanoparticle volume percentage and the Ra. When the loading of the nanoparticles is raised, there is a corresponding rise in the temperature distribution within the cavity. The increase in magnetic field effects does not seem to influence the distribution of the temperatures substantially.
Li et al. (2020)	Microchannel with triangular cavities and rectangular fins	Impact of micro fins.	Numerical	The micro fins' acceleration, disturbance, and separation effects contributed to increased pressure drop. This situation might be rectified by further optimizing the structure.
Sheremet et al. (2017)	Under the influence of Brownian diffusion and thermophoresis, a nanofluid is based on water inside two entrapped triangular cavities.	Effect of the Rayleigh number and buoyancy-ratio parameter.	Numerical	The presence of non-uniform distributions of nanoparticles inside cavities is reflected by an increase in the Rayleigh number and the buoyancy-ratio parameter.
Gangawane et al. (2019)	A triangular block drives a cavity with a square lid and has a constant heat flow. A change in the placement of the block impacts this cavity.	The effect of the changes in the block's location along the vertical centerline.	Numerical	Compared to the other two (Ly = 0.25 and 0.75), the heat transfer rates are more significant for the centered block location (Ly = 0.5). The Nusselt number exhibits a decreasing trend with increasing Ri for any given obstruction.
Bilal et al. (2020)	A heated square cylinder is positioned in the middle of a triangle cage that contains a viscous substance. This material interacts with it.	Effect of Rayleigh number.	Numerical	The magnitude of the velocity at every position inside the cavity increases for the intensifying values of the Rayleigh number.
Zadeh et al. (2020)	Square enclosure with two solid triangular walls.	Effect of the triangular blocks and position of triangular walls.	Numerical	The inclusion of the triangular blocks results in an increase in the rate of heat transmission overall. The standard deviation of the Nusselt number rises whenever the R_k value goes down. When the triangle walls are turned around, they create an environment in which the heat transmission rate is reduced overall.
Yao et al. (2021)	Microchannel with triangular cavity and rib.	Optimize design variables (cavity height, rib height, and Reynold number).	Numerical	Because there was a high synergy between the velocity field and temperature gradient, Case 4 had the best thermal performance possible (e1 = 0.0572 mm, e2 = 0.0224 mm). This was determined by using a thermal enhancement factor of 1.2305.
Wijayanta (2021)	Natural convection in a cavity.	Effect of Prandtl number.	Numerical	It is discovered that there are two different types of circulation cells for low Pr ($0.026 \leq Pr \leq 0.7$). A primary circulation cell formed in the cavity's center, and a second circulation cell developed at the cavity's bottom corners. A high Pr ($0.7 \leq Pr \leq 1000$) causes the secondary circulation to disappear completely, weaker than the central circulation.
Shahid et al. (2021)	Heated lid-driven right triangular cavity.	Effect of Gr.	Numerical	As the water's specific gravity (Gr) rises, the buoyancy forces will also. Because of this, the influence of natural convection is far more significant than the effect of induced convection. In this particular instance, there is shown to be a rise in the typical Nusselt number.
Shekaramiz et al. (2021)	A triangular chamber with a hot wavy wall.	Magnetic field changes may be described using the Hartmann number (Ha), the	Numerical	The number of undulations has a considerable impact on the rate of heat transmission. In addition, the relationship between the Nusselt

(*continued on next page*)

Table 4 (*continued*)

Authors (year)	Structure	Examined variables	Study method	Results / Impacts
		Rayleigh number (Ra), the undulation number (n), and the inclination angle.		number and the undulation number is inverse, while the relationship between the Nusselt number and the Rayleigh number is direct. In addition, there is an inverse relationship between the heat transfer rate and the overall entropy creation.
Xiong et al. (2021)	A primarily triangular wall heats a triangular hollow with a lid.	Effect of Richardson number and Hartmann number.	Numerical	While an increase in the Nusselt number causes the Richardson number to go in the opposite direction, an increase in the Hartmann number causes the Richardson number to go in the other order.
Sarlak et al. (2023)	Nanofluid in a triangular cavity.	The angle of attack, the fluid injection, and the volume percentage of the nanoparticles.	Numerical	When the angle of attack is larger, the cavity temperature inclines become more pronounced. Increasing heat transmission by increasing solid nanoparticle volume fraction (φ) and adding fluid injection into the cavity is feasible. When the value φ of is increased, the viscosity and density of the cooling fluid increase, resulting in a more significant rate at which momentum is lost.

improvement of thermal conductivity. According to previous research on the spherical cavity, the boundary impact may significantly impact the cavity growth reaction when the outside-to-inside radius ratio is insignificant. In the case of PCM with a hollow fin, melting time is cut by a factor of 14 compared to a setup without fins. The ratio of particle radius to cavity radius and the permeability parameter negatively affects the non-dimensional velocity.

- Square Containers: Housing NEPCMs can be done simply using square containers. They may be packed closely together, making them ideal for applications where space efficiency is crucial. Additionally, square containers make it easier for nanoparticles to disperse uniformly within the PCM, improving heat conductivity. However, the square shape of the containers may cause stress concentration, which could compromise the material's structural integrity. To minimize this problem, careful design and material choices are required. Results from the experiments of the square cavity showed that an increase in Aspect Ratio (AR) lengthens the total melting time for both left and bottom wall heating circumstances. Additionally, when the thermal conductivity ratio is low, the influence of the partition thickness on heat transport is particularly noticeable. It is also observed that the heat and flow structures are susceptible to the magnetic field intensity, Rayleigh number, and ferroparticle concentration in the base fluid.
- Trapezoidal Containers: Although less frequently studied, trapezoidal containers offer a chance for novel thermal conductivity improvements in NEPCMs. Their asymmetrical form increases the surface area that comes into contact with the PCM, potentially facilitating more effective heat transfer. Trapezoidal containers are less useful for particular applications because their use may necessitate specific production techniques. To improve the design and production of trapezoidal containers, more research is required. Based on the findings of the associated studies, the rate of heat transfer rises with increasing levels of the Rayleigh number and a constant aspect ratio in a trapezoidal cavity. The rate of heat transmission reduces as the aspect ratio increases. The heat transfer coefficient increases with the Rayleigh number and decreases with the Richardson number. The average Nusselt number increases as the volume proportion of nanoparticles increases. Slowing the flow inside the cavity reduces heat transmission as the Hartmann number rises.
- Containers with triangular geometry provide exciting opportunities for improving the thermal characteristics of NEPCMs. Similar to trapezoidal containers, its distinct shape can expand the PCM's contact area, which might enhance thermal conductivity. However, similar to trapezoidal containers, difficulties with manufacture and dispersion could occur. In order to successfully maximize the advantages of triangular containers, researchers need to investigate novel ways. The research on the triangular cavity has shown that the Richardson number increases as a function of the Nusselt number, whereas the Hartmann number increases in the opposite direction. The addition of triangular pieces further improves the heat transmission rate. The Rayleigh number and the buoyancy-ratio parameter rise when nanoparticles are distributed unevenly inside a cavity.

The choice of container geometry is crucial for improving the thermal characteristics of NEPCMs, particularly their thermal conductivity. Although simple, spherical containers may have difficulties with nanoparticle dispersion. Square containers offer a balanced approach, although stress concentration must be carefully taken into account. Triangular and trapezoidal containers have particular advantages, although more study and development are needed.

In the end, the container geometry should be chosen in accordance with the particular application, spatial limitations, and dispersion strategies. To realize the full potential of these container geometries in improving NEPCMs for TES and management, researchers should carry out further research and refinement in the design, production, and modeling of these container geometries.

4. Conclusions

This work looked at the most recent research on heat transport efficiency in cavities. The literature on natural and coupled heat convection and fluid flow is reviewed, including computational and experimental studies for various geometries (spherical, square, trapezoidal, and triangular), working fluids, heating sources, and boundary conditions. Porosity, an external magnetic field, and conjugate heat transport were also considered. The key findings may be summed up as follows:

- The thermal exchange rate improves noticeably when the Ra is raised; with a value of 10^7, it is at its highest and most efficient.
- With rising starting gas pressure and, thus, lowering p, the extreme pressure value at the limited point drops monotonically.
- The average temperature within the heated element may be lowered by increasing the surface emissivity or by spinning the element rapidly.
- The cooling rate is increased, and the time needed for complete solidification is decreased, thanks to the nanoparticles in the base fluid.

- Thermophoresis, in which nanoparticles move from the heated wall to the cold nanofluid flow, is amplified as the Reynolds number increases.
- Increasing the heated area of the lower flat fin improves the heat transfer rate, whereas increasing the value of Ra and the solid volume percentage of nanoparticles reduces it.
- Radiation blockage affects the path of hot particles and changes the anticipated radiative amount. Optical thickness has a role in the rapid cooling of a medium.
- Heat transport is most affected by partition thickness when the ratio of thermal conductivities is low.
- Heat transmission is enhanced When the Rayleigh number is high, and the Richardson number is low.
- For both fluids and solids, the Rayleigh number and the local Nusselt number show a dominating improvement, but the average Nusselt number decreases with an increase in the heating domains.
- The heat transmission rate also depends heavily on the number of undulations. Nusselt number is closely connected to the Rayleigh number and has an inverse relationship to the undulation number.
- Ra-dependent increase in average velocity across the cavity.
- Ra increases the heat transfer rate by 2.32 and the entropy generation by 14.17.

5. Recommendation for future work

When the external wind is absent or weak, the cavity is heated and cooled mostly through radiation and free convection. Reducing heat loss boosts thermal efficiency in the cavity and the whole system. Before this, knowledge of radiation and free convection was crucial. As a result, much research went into them. Studies often position cavities on the side or bottom. This could not accommodate the expanding uses for upward-facing cavities, such as in solar thermo-electrical generation units, solar beam-down tower units, and the scanning of material behaviours at the surface level. Electronics might benefit from chambers that face upward. For the following reasons, some of the many pending and significant cases that bear mentioning below:

1. Look at different container geometries besides spheres, squares, trapezoids, and triangles to find possible forms that could improve thermal conductivity even further.
2. Develop cutting-edge fabrication methods to produce containers with intricate geometries with accuracy and reliability.
3. Continue your research into more effective nanoparticle dispersion techniques, especially for containers with unusual geometries, to ensure uniform distribution within NEPCMs.
4. To comprehend how nanoparticles affect the improvement of thermal conductivity, investigate the interactions between nanoparticles and container materials.
5. To obtain synergistic effects on thermal conductivity, look into the utilization of multi-phase NEPCMs that combine several types of nanoparticles or hybrid architectures.
6. Examine the long-term stability and durability of NEPCMs in containers, taking into account any potential deterioration of the nanoparticles and the materials used to make the containers.
7. Identify the economic viability and total energy efficiency of NEPCM systems with various container geometries by taking into account elements like heat transfer rates and energy storage/release dynamics.
8. Future studies may find that the phase change procedure involves turbulent free convection, which would match the laminar condition seen in the cavity in the present study.
9. The existence of nano plastic or microplastic in cavity fluids is seldom considered. Examine the hydraulic and thermal effects of a cavity containing two im-miscible liquids (air and water) is important.

Author contributions

Conceptualization, F.L.R. and A.A.; Methodology, F.L.R. H.I.M., and M.A.Al-O.; Software, H.I.M.; Validation, F.L.R., M.A.Al-O. and P.T.; Formal analysis, S.A. and A.A.; Investigation, F.L.R.; Resources, A.D. and A.A.; Data curation, F.L.R, A.D. and A.A.; Writing – original draft preparation, F.L.R., H.I.M., A.D., M.A.Al-O. and A.A.; Writing – review & editing, F.L.R., H.I.M., A.D., M.A.Al-O., P.T., S.A. and A.A.; Visualization, F.L.R.; Supervision, A.D. and F.L.R.; Project administration, F.L.R. A.A., and A.D. All authors have read and agreed to the published version of the manuscript.

Institutional review board statement

Not applicable.

Funding

This research received no external funding.

Declaration of Competing Interest

The authors declare that they have no known competing financial interests or personal relationships that could have appeared to influence the work reported in this paper.

Data Availability

No data was used for the research described in the article.

Acknowledgments

The financial support of Kerbala University and University of Warith Al-Anbiyaa in Iraq is gratefully acknowledged.

Informed consent statement

Not applicable.

References

Afrand, M., Pordanjani, A.H., Aghakhani, S., Oztop, H.F., Abu-Hamdeh, N., 2020. Free convection and entropy generation of a nanofluid in a tilted triangular cavity exposed to a magnetic field with sinusoidal wall temperature distribution considering radiation effects. Int. Commun. Heat. Mass Transf. 112, 104507 https://doi.org/10.1016/j.icheatmasstransfer.2020.104507.

Alfellag, M.A., Ahmed, H.E., Fadhil, O.T., Sh, Kherbeet, A., 2019. Optimal hydrothermal design of microchannel heat sink using trapezoidal cavities and solid/slotted oval pins. Appl. Therm. Eng. 158, 113765 https://doi.org/10.1016/j.applthermaleng.2019.113765.

Alnaqi, A.A., Aghakhani, S., Pordanjani, A.H., Bakhtiari, R., Asadi, A., Tran, M.D., 2019. Effects of magnetic field on the convective heat transfer rate and entropy generation of a nanofluid in an inclined square cavity equipped with a conductor fin: Considering the radiation effect. Int J. Heat. Mass Transf. 133, 256–267. https://doi.org/10.1016/j.ijheatmasstransfer.2018.12.110.

Alshare, A., Abderrahmane, A., Guedri, K., Younis, O., Fayz-Al-Asad, M., Ali, H.M., Al-Kouz, W., 2022. Hydrothermal and entropy investigation of nanofluid natural convection in a lid-driven Cavity concentric with an elliptical cavity with a wavy boundary heated from below. Nanomaterials 12, 1392. https://doi.org/10.3390/nano12091392.

Alvarado-Juárez, R., Montiel-González, M., Villafán-Vidales, H.I., Estrada, C.A., Flores-Navarrete, J., 2020. Experimental and numerical study of conjugate heat transfer in an open square-cavity solar receiver. Int. J. Therm. Sci. 156, 106458 https://doi.org/10.1016/j.ijthermalsci.2020.106458.

Azimikivi, H., Purmahmud, N., Mirzaee, I., 2020. Rib shape and nanoparticle diameter effects on natural convection heat transfer at low turbulence two-phase flow of AL2O3-water nanofluid inside a square cavity: Based on Buongiorno's two-phase model. Therm. Sci. Eng. Prog. 20, 100587 https://doi.org/10.1016/j.tsep.2020.100587.

Bhatti, M.M., Bég, O.A., Abdelsalam, S.I., 2022. Computational framework of magnetized MgO–Ni/water-based stagnation nanoflow past an elastic stretching surface: application in solar energy coatings. Nanomaterials 12, 1049. https://doi.org/10.3390/nano12071049.

Bilal, S., Mahmood, R., Majeed, A.H., Khan, I., Nisar, K.S., 2020. Finite element method visualization about heat transfer analysis of Newtonian material in triangular cavity with square cylinder. J. Mater. Res. Technol. 9, 4904–4918. https://doi.org/10.1016/j.jmrt.2020.03.010.

Chen, S., Gong, W., Yan, Y., 2018. Conjugate natural convection heat transfer in an open-ended square cavity partially filled with porous media. Int J. Heat. Mass Transf. 124, 368–380. https://doi.org/10.1016/j.ijheatmasstransfer.2018.03.084.

Cho, C.C., 2020. Effects of porous medium and wavy surface on heat transfer and entropy generation of Cu-water nanofluid natural convection in square cavity containing partially-heated surface. Int. Commun. Heat. Mass Transf. 119. https://doi.org/10.1016/j.icheatmasstransfer.2020.104925.

Corcione, M., 2003. Effects of the thermal boundary conditions at the sidewalls upon natural convection in rectangular enclosures heated from below and cooled from above. Int. J. Therm. Sci. 42, 199–208. https://doi.org/10.1016/S1290-0729(02)00019-4.

Dabiri, S., Khodabandeh, E., Poorfar, A.K., Mashayekhi, R., Toghraie, D., Abadian Zade, S.A., 2018. Parametric investigation of thermal characteristic in trapezoidal cavity receiver for a linear Fresnel solar collector concentrator. Energy 153, 17–26. https://doi.org/10.1016/j.energy.2018.04.025.

Datta, A., Sharma, V., Sanyal, D., Das, P., 2019. A conjugate heat transfer analysis of performance for rectangular microchannel with trapezoidal cavities and ribs. Int. J. Therm. Sci. 138, 425–446. https://doi.org/10.1016/j.ijthermalsci.2018.12.020.

De, A.K., Dalal, A., 2006. A numerical study of natural convection around a square, horizontal, heated cylinder placed in an enclosure. Int J. Heat. Mass Transf. 49, 4608–4623. https://doi.org/10.1016/j.ijheatmasstransfer.2006.04.020.

de Souza, J.F.V.G., Henríquez, J.R., de Lira Junior, J.C., de Brito Filho, J.P., 2020. Parametric analysis of the solidification of nanofluids in spherical cavities. Powder Technol. 359, 47–58. https://doi.org/10.1016/j.powtec.2019.09.065.

Dhaidan, N.S., Khodadadi, J.M., 2015. Melting and convection of phase change materials in different shape containers: a review. Renew. Sustain. Energy Rev. 43, 449–477. https://doi.org/10.1016/j.rser.2014.11.017.

Dhaidan, Nabeel S., Kokz, Samer A., Rashid, Farhan Lafta, Hussein, Ahmed Kadhim, Younis, Obai, Al-Mousawi, Fadhel Noraldeen, 2022. Review of solidification of phase change materials dispersed with nanoparticles in different containers. J. Energy Storage Volume 51, 104271. https://doi.org/10.1016/j.est.2022.104271.

Djeumegni, J.S., Lazard, M., Dez, V., Le, Kamdem, H.T.T., 2020. Radiative heat transfer in a 2D semi-transparent gray medium with a centered inner square cavity. Int J. Heat. Mass Transf. 149. https://doi.org/10.1016/j.ijheatmasstransfer.2019.119209.

Duan, J., Xiong, Y., Yang, D., 2019. Melting behavior of phase change material in honeycomb structures with different geometrical cores. Energies 12 (15), 2920. https://doi.org/10.3390/en12152920.

Ebrahimi, N., Ashtiani, H.A.D., Toghraie, D., 2023. Lattice Boltzmann method for mixed convection of nanofluid two-phase flow in a trapezoidal-shaped sinusoidal cavity by considering Brownian motion. Eng. Anal. Bound Elem. 152, 194–213. https://doi.org/10.1016/j.enganabound.2023.03.040.

El-Sapa, S., 2020. Effect of permeability of Brinkman flow on thermophoresis of a particle in a spherical cavity. Eur. J. Mech. -B/Fluids 79, 315–323. https://doi.org/10.1016/j.euromechflu.2019.09.017.

Fan, L.-W., Zhu, Z.-Q., Zeng, Y., Ding, Q., Liu, M.-J., 2016. Unconstrained melting heat transfer in a spherical container revisited in the presence of nano-enhanced phase change materials (NePCM). Int J. Heat. Mass Transf. 95, 1057–1069. https://doi.org/10.1016/j.ijheatmasstransfer.2016.01.013.

Fayz-Al-Asad, M., Nur Alam, M., Ahmad, H., Sarker, M.M.A., Alsulami, M.D., Gepreel, K. A., 2021. Impact of a closed space rectangular heat source on natural convective flow through triangular cavity. Results Phys. 23, 104011 https://doi.org/10.1016/j.rinp.2021.104011.

Fukusako, S., Yamada, M., 1999. Melting heat transfer inside ducts and over external bodies. Exp. Therm. Fluid Sci. 19, 93–117. https://doi.org/10.1016/S0894-1777(99)00011-4.

Gangawane, K.M., Manikandan, B., 2017. Laminar natural convection characteristics in an enclosure with heated hexagonal block for non-Newtonian power law fluids. Chin. J. Chem. Eng. 25, 555–571. https://doi.org/10.1016/j.cjche.2016.08.028.

Gangawane, K.M., Oztop, H.F., Ali, M.E., 2019. Mixed convection in a lid-driven cavity containing triangular block with constant heat flux: Effect of location of block. Int J. Mech. Sci. 152, 492–511. https://doi.org/10.1016/j.ijmecsci.2019.01.020.

Gowda, B.M.K., Rajagopal, M.S., Aswatha, Seetharamu, K.N., 2019. Heat transfer in a side heated trapezoidal cavity with openings. Eng. Sci. Technol., Int. J. 22, 153–167. https://doi.org/10.1016/j.jestch.2018.04.017.

Ha, M.Y., Kim, I.-K., Yoon, H.S., Yoon, K.S., Lee, J.R., Balachandar, S., Chun, H.H., 2002. Two-dimensional and unsteady natural convection in a horizontal enclosure with a square body. Numer. Heat. Transf. A Appl. 41, 183–210. https://doi.org/10.1080/104077802317221393.

Hamid, M., Usman, M., Khan, Z.H., Haq, R.U., Wang, W., 2019. Heat transfer and flow analysis of Casson fluid enclosed in a partially heated trapezoidal cavity. Int. Commun. Heat. Mass Transf. 108, 104284 https://doi.org/10.1016/j.icheatmasstransfer.2019.104284.

Haq, R.U., Soomro, F.A., Öztop, H.F., Mekkaoui, T., 2019. Thermal management of water-based carbon nanotubes enclosed in a partially heated triangular cavity with heated cylindrical obstacle. Int J. Heat. Mass Transf. 131, 724–736. https://doi.org/10.1016/j.ijheatmasstransfer.2018.11.090.

Haq, R.U., Shah, S.S., Algehyne, E.A., Tlili, I., 2020. Heat transfer analysis of water based SWCNTs through parallel fins enclosed by square cavity. Int. Commun. Heat. Mass Transf. 119. https://doi.org/10.1016/j.icheatmasstransfer.2020.104797.

Hong, Y., Ding, S., Wu, W., Hu, J., Voevodin, A.A., Gschwender, L., Snyder, E., Chow, L., Su, M., 2010. Enhancing heat capacity of colloidal suspension using nanoscale encapsulated phase-change materials for heat transfer. ACS Appl. Mater. Interfaces 2 (6), 1685–1691. https://doi.org/10.1021/am100204b.

Hussain, S., Ismael, M.A., Chamkha, A.J., 2020. Impinging jet into an open trapezoidal cavity partially filled with a porous layer. Int. Commun. Heat. Mass Transf. 118, 104870 https://doi.org/10.1016/j.icheatmasstransfer.2020.104870.

Iachachene, F., Haddad, Z., Oztop, H.F., Abu-Nada, E., 2019. Melting of phase change materials in a trapezoidal cavity: orientation and nanoparticles effects. J. Mol. Liq. 292, 110592 https://doi.org/10.1016/j.molliq.2019.03.051.

Ibrahim, W., Hirpho, M., 2021. Finite element analysis of mixed convection flow in a trapezoidal cavity with non-uniform temperature. Heliyon 7. https://doi.org/10.1016/j.heliyon.2021.e05933.

Irwan, M.A.M., Azwadi, C.N., Asako, Y., 2019. Review on numerical simulations for solidification & melting of nano-enhanced phase change materials (NEPCM). In: IOP Conference Series: Earth and Environmental Science, Vol. 268. IOP Publishing,. https://doi.org/10.1088/1755-1315/268/1/012114.

Javed, T., Siddiqui, M.A., 2018. Effect of MHD on heat transfer through ferrofluid inside a square cavity containing obstacle/heat source. Int. J. Therm. Sci. 125, 419–427. https://doi.org/10.1016/j.ijthermalsci.2017.12.009.

Jiao, D., Gao, J., Zhang, L., Deng, X., Zang, Q., Xu, G., Dong, R., Liu, T., Zhang, S., 2023. Theoretical and experimental study on vibration sensitivity of a transportable spherical optical reference cavity with multi-channel. Opt. Commun. 537, 129459 https://doi.org/10.1016/j.optcom.2023.129459.

Khan, Z.H., Makinde, O.D., Hamid, M., Haq, R.U., Khan, W.A., 2020. Hydromagnetic flow of ferrofluid in an enclosed partially heated trapezoidal cavity filled with a porous medium. J. Magn. Magn. Mater. 499, 166241 https://doi.org/10.1016/j.jmmm.2019.166241.

Khan, Z.H., Hamid, M., Khan, W.A., Sun, L., Liu, H., 2021. Thermal non-equilibrium natural convection in a trapezoidal porous cavity with heated cylindrical obstacles. Int. Commun. Heat. Mass Transf. 126, 105460 https://doi.org/10.1016/j.icheatmasstransfer.2021.105460.

Khatamifar, M., Lin, W., Dong, L., 2021. Transient conjugate natural convection heat transfer in a differentially-heated square cavity with a partition of finite thickness and thermal conductivity. Case Stud. Therm. Eng. 25. https://doi.org/10.1016/j.csite.2021.100952.

Kumara, V.V, Pavan, K.S., Reddy, A.S., Sharath, B.S., 2023. Effect of aspect ratio on the onset of natural convection in porous trapezoidal enclosures. Mater. Today Proc. https://doi.org/10.1016/j.matpr.2023.05.008.

Lee, J.R., Ha, M.Y., Balachandar, S., Yoon, H.S., Lee, S.S., 2004. Natural convection in a horizontal layer of fluid with a periodic array of square cylinders in the interior. Phys. Fluids 16, 1097–1117. https://doi.org/10.1063/1.1649989.

Li, Y.F., Xia, G.D., Ma, D.D., Yang, J.L., Li, W., 2020. Experimental investigation of flow boiling characteristics in microchannel with triangular cavities and rectangular fins. Int J. Heat. Mass Transf. 148, 119036 https://doi.org/10.1016/j.ijheatmasstransfer.2019.119036.

Liu, M.-J., Fan, L.-W., Zhu, Z.-Q., Feng, B., Zhang, H.-C., Zeng, Y., 2016. A volume-shrinkage-based method for quantifying the inward solidification heat transfer of a phase change material filled in spherical capsules. Appl. Therm. Eng. 108, 1200–1205. https://doi.org/10.1016/j.applthermaleng.2016.08.027.

Lohrasbi, S., Bandpy, M.G., Ganji, D.D., 2016. Response surface method optimization of V-shaped fin assisted latent heat thermal energy storage system during discharging process. Alex. Eng. J. 55, 2065–2076. https://doi.org/10.1016/j.aej.2016.07.004.

Lohrasbi, S., Gorji-Bandpy, M., Ganji, D.D., 2017. Thermal penetration depth enhancement in latent heat thermal energy storage system in the presence of heat pipe based on both charging and discharging processes. Energy Convers. Manag 148, 646–667. https://doi.org/10.1016/j.enconman.2017.06.034.

Lotfy, K., 2017. A novel solution of fractional order heat equation for photothermal waves in a semiconductor medium with a spherical cavity. Chaos Solitons Fractals 99, 233–242. https://doi.org/10.1016/j.chaos.2017.04.017.

Mahdi, J.M., Lohrasbi, S., Ganji, D.D., Nsofor, E.C., 2018. Accelerated melting of PCM in energy storage systems via novel configuration of fins in the triplex-tube heat exchanger. Int J. Heat. Mass Transf. 124, 663–676. https://doi.org/10.1016/j.ijheatmasstransfer.2018.03.095.

Mahdi, J.M., Lohrasbi, S., Ganji, D.D., Nsofor, E.C., 2019. Simultaneous energy storage and recovery in the triplex-tube heat exchanger with PCM, copper fins and Al2O3 nanoparticles. Energy Convers. Manag 180, 949–961. https://doi.org/10.1016/j.enconman.2018.11.038.

Maneengam, A., Laidoudi, H., Abderrahmane, A., Rasool, G., Guedri, K., Weera, W., Younis, O., Bouallegue, B., 2022. Entropy generation in 2D lid-driven porous container with the presence of obstacles of different shapes and under the influences of Buoyancy and Lorentz Forces. Nanomaterials 12, 2206. https://doi.org/10.3390/nano12132206.

Mebarek-Oudina, F., Fares, R., Aissa, A., Lewis, R.W., Abu-Hamdeh, N, H., 2021. Entropy and convection effect on magnetized hybrid nano-liquid flow inside a trapezoidal cavity with zigzagged wall. Int. Commun. Heat. Mass Transf. 125, 105279 https://doi.org/10.1016/j.icheatmasstransfer.2021.105279.

Meghari, Z., Bouhal, T., Benghoulam, M., El Rhafiki, T., Mohammed, O.J., 2021. Numerical simulation of a phase change material in a spherical capsule with a hollow fin. J. Energy Storage 43, 103024. https://doi.org/10.1016/j.est.2021.103024.

Mikhailenko, S.A., Sheremet, M.A., Mohamad, A.A., 2018. Convective-radiative heat transfer in a rotating square cavity with a local heat-generating source. Int J. Mech. Sci. 142–143. https://doi.org/10.1016/j.ijmecsci.2018.05.030.

Mohebbi, R., lakzayi, H., Rasam, H., 2020. Numerical simulation of conjugate heat transfer in a square cavity consisting the conducting partitions by utilizing lattice Boltzmann method. Phys. A: Stat. Mech. Appl. 546, 123050 https://doi.org/10.1016/j.physa.2019.123050.

Momoniat, E., Harley, C., Herbst, R.S., 2023. Effects of extended surfaces on heat transfer in buoyancy-driven flow in a square cavity. Results Eng. 18, 101190 https://doi.org/10.1016/j.rineng.2023.101190.

Mondal, P., Mahapatra, T.R., 2021. MHD double-diffusive mixed convection and entropy generation of nanofluid in a trapezoidal cavity. Int J. Mech. Sci. 208, 106665 https://doi.org/10.1016/j.ijmecsci.2021.106665.

Morenko, I.V., 2020. Numerical simulation of the propagation of pressure waves in water during the collapse of a spherical air cavity. Ocean Eng. 215, 107905 https://doi.org/10.1016/j.oceaneng.2020.107905.

Muhammad, S., Andrzejczyk, R., 2023. A review of phase change materials and heat enhancement methodologies. WIREs Energy Environ. 12, e467 https://doi.org/10.1002/wene.467.

Nayak, J., Agrawal, M., Mishra, S., Sahoo, S.S., Swain, R.K., Mishra, A., 2018. Combined heat loss analysis of trapezoidal shaped solar cooker cavity using computational approach. Case Stud. Therm. Eng. 12, 94–103. https://doi.org/10.1016/j.csite.2018.03.009.

Ouertatani, N., Cheikh, N., Ben, Beya, B., Ben, Lili, T., 2008. Numerical simulation of two-dimensional Rayleigh–Bénard convection in an enclosure. Comptes Rendus Mécanique 336, 464–470. https://doi.org/10.1016/j.crme.2008.02.004.

Pan, M., Zhong, Y., Xu, Y., 2018. Numerical investigation of fluid flow and heat transfer in a plate microchannel heat exchanger with isosceles trapezoid-shaped reentrant cavities in the sidewall. Chem. Eng. Process. - Process. Intensif. 131, 178–189. https://doi.org/10.1016/j.cep.2018.07.018.

Qasem, N.A.A., Abderrahmane, A., Khetib, Y., Rawa, M., Abdulkadhim, A., Eldin, S.M., Younis, O., 2023. Mixed convection within trapezoidal-wavy enclosure filled with nano-encapsulated phase change material: effect of magnetohydrodynamics and wall waviness. Case Stud. Therm. Eng. 42, 102726 https://doi.org/10.1016/j.csite.2023.102726.

Qin, Y., Chen, K., Zhang, H., Luo, X., Liang, S., Tian, C., Wang, J., Zhang, L., 2019. Structure-property correlation of poly (ethylene glycol) based form stable phase change materials with different crosslinking structure. Sol. Energy Mater. Sol. Cells 203, 110192. https://doi.org/10.1016/j.solmat.2019.110192.

Rashid, F.L., Basem, A., Khalaf, F.A.A., Abbas, M.H., Hashim, A., 2022a. Recent Breakthroughs and Improvements in Phase Change Material Melting in a Triple-Tube Thermal Storage Unit. Rev. Des. Compos. Et. Des. Mater. Av. 32, 295. https://doi.org/10.18280/rcma.320605.

Rashid, F.L., Al-Obaidi, M.A., Dulaimi, A., Bahlol, H.Y., Hasan, A., 2023a. Recent advances, development, and impact of using phase change materials as thermal energy storage in different solar energy systems: a review. Design 7, 66. https://doi.org/10.3390/designs7030066.

Rashid, F.L., Al-Obaidi, M.A., Dulaimi, A., Bahlol, H.Y., Hasan, A., 2023c. Recent advances, development, and impact of using phase change materials as thermal energy storage in different solar energy systems: a review. Designs 7 (3), 66. https://doi.org/10.3390/designs7030066.

Rashid, F.L., Hussein, A.K., Malekshah, E.H., Abderrahmane, A., Guedri, K., Younis, O., 2022b. Review of heat transfer analysis in different cavity geometries with and without nanofluids. Nanomaterials 12, 2481. https://doi.org/10.3390/nano12142481.

Rashid, F.L., Al-Obaidi, M.A., Dulaimi, A., Bernardo, L.F.A., Eleiwi, M.A., Mahood, H.B., Hashim, A., 2023d. A review of recent improvements, developments, effects, and challenges on using phase-change materials in concrete for thermal energy storage and release. J. Compos. Sci. 7 (9), 352. https://doi.org/10.3390/jcs7090352.

Rashid, F.L., Rahbari, A., Ibrahem, R.K., Talebizadehsardari, P., Basem, A., Kaood, A., Mohammed, H.I., Abbas, M.H., Al-Obaidi, M.A., 2023b. Review of solidification and melting performance of phase change materials in the presence of magnetic field, rotation, tilt angle, and vibration. J. Energy Storage 67, 107501. https://doi.org/10.1016/j.est.2023.107501.

Rashid, U., Lu, D., Iqbal, Q., 2023. Nanoparticles impacts on natural convection nanofluid flow and heat transfer inside a square cavity with fixed a circular obstacle. Case Stud. Therm. Eng. 44, 102829 https://doi.org/10.1016/j.csite.2023.102829.

Regin, A.F., Solanki, S.C., Saini, J.S., 2008. Heat transfer characteristics of thermal energy storage system using PCM capsules: a review. Renew. Sustain. Energy Rev. 12, 2438–2458. https://doi.org/10.1016/j.rser.2007.06.009.

Sarlak, R., Abed, A.M., Akbari, O.A., Marzban, A., Baghaei, S., Bayat, M., 2023. Numerical investigation of natural convection heat transfer of water/ SWCNT nanofluid flow in a triangular cavity with cold fluid injection. Prog. Nucl. Energy 155, 104513. https://doi.org/10.1016/j.pnucene.2022.104513.

Sevastyanov, G.M., 2021. Adiabatic heating effect in elastic-plastic contraction/ expansion of spherical cavity in isotropic incompressible material. Eur. J. Mech. -A/ Solids 87, 104223. https://doi.org/10.1016/j.euromechsol.2021.104223.

Shah, S.S., Haq, R.U., Al-Kouz, W., 2021. Mixed convection analysis in a split lid-driven trapezoidal cavity having elliptic shaped obstacle. Int. Commun. Heat. Mass Transf. 126, 105448 https://doi.org/10.1016/j.icheatmasstransfer.2021.105448.

Shahid, H., Yaqoob, I., Khan, W.A., Rafique, A., 2021. Mixed convection in an isosceles right triangular lid driven cavity using multi relaxation time lattice Boltzmann method. Int. Commun. Heat. Mass Transf. 128, 105552 https://doi.org/10.1016/j.icheatmasstransfer.2021.105552.

Shekaramiz, M., Fathi, S., Ataabadi, H.A., Kazemi-Varnamkhasti, H., Toghraie, D., 2021. MHD nanofluid free convection inside the wavy triangular cavity considering periodic temperature boundary condition and velocity slip mechanisms. Int. J. Therm. Sci. 170, 107179 https://doi.org/10.1016/j.ijthermalsci.2021.107179.

Sheremet, M.A., Revnic, C., Pop, I., 2017. Natural convective heat transfer through two entrapped triangular cavities filled with a nanofluid: Buongiorno's mathematical model. Int J. Mech. Sci. 133, 484–494. https://doi.org/10.1016/j.ijmecsci.2017.09.010.

Sheremet, M.A., Roşca, N.C., Roşca, A.V., Pop, I., 2018. Mixed convection heat transfer in a square porous cavity filled with a nanofluid with suction/injection effect. Comput. Math. Appl. 76, 2665–2677. https://doi.org/10.1016/j.camwa.2018.08.069.

Shew, C.-Y., Yoshikawa, K., 2023. Crowding effect on the alignment of rod molecules confined in a spherical cavity. Chem. Phys. Lett. 819, 140437 https://doi.org/10.1016/j.cplett.2023.140437.

Solomon, A.B., van Rooyen, J., Rencken, M., Sharifpur, M., Meyer, J.P., 2017. Experimental study on the influence of the aspect ratio of square cavity on natural convection heat transfer with Al2O3/Water nanofluids. Int. Commun. Heat. Mass Transf. 88, 254–261. https://doi.org/10.1016/j.icheatmasstransfer.2017.09.007.

Soomro, F.A., Haq, R.U., Algehyne, E.A., Tlili, I., 2020. Thermal performance due to magnetohydrodynamics mixed convection flow in a triangular cavity with circular obstacle. J. Energy Storage 31, 101702. https://doi.org/10.1016/j.est.2020.101702.

Tiji, M.E., Al-Azzawi, W.K., Mohammed, H.I., Dulaimi, A., Rashid, F.L., Mahdi, J.M., Majdi, H.S., Talebizadehsardari, P., Ali, H.M., 2022. Thermal management of the melting process in a latent heat triplex tube storage system using different configurations of frustum tubes. J. Nanomater 2022. https://doi.org/10.1155/2022/7398110.

Tseng, Y.M., Keh, H.J., 2020. Thermophoretic motion of an aerosol sphere in a spherical cavity. Eur. J. Mech. -B/Fluids 81, 93–104. https://doi.org/10.1016/j.euromechflu.2019.12.010.

Wang, Y., Qin, G., 2018. An improved time-splitting method for simulating natural convection heat transfer in a square cavity by Legendre spectral element approximation. Comput. Fluids 174. https://doi.org/10.1016/j.compfluid.2018.07.013.

Wei, G., Wang, G., Xu, C., Ju, X., Xing, L., Du, X., Yang, Y., 2018. Selection principles and thermophysical properties of high temperature phase change materials for thermal energy storage: A review. Renew. Sustain. Energy Rev. 81, 1771–1786. https://doi.org/10.1016/j.rser.2017.05.271.

Welhezi, H., Ben-Cheikh, N., Ben-Beya, B., 2020. Numerical analysis of natural convection between a heated cube and its spherical enclosure. Int. J. Therm. Sci. 150, 105828 https://doi.org/10.1016/j.ijthermalsci.2019.02.003.

Wijayanta, A.T., 2021. Numerical solution strategy for natural convection problems in a triangular cavity using a direct meshless local Petrov-Galerkin method combined with an implicit artificial-compressibility model. Eng. Anal. Bound Elem. 126, 13–29. https://doi.org/10.1016/j.enganabound.2021.02.006.

Xie, S., Wu, W., 2023. Effect of aspect ratio on PCM melting behavior in a square cavity. Int. Commun. Heat. Mass Transf. 143, 106708 https://doi.org/10.1016/j.icheatmasstransfer.2023.106708.

Xiong, P.Y., Hamid, A., Iqbal, K., Irfan, M., Khan, M., 2021. Numerical simulation of mixed convection flow and heat transfer in the lid-driven triangular cavity with different obstacle configurations. Int. Commun. Heat. Mass Transf. 123, 105202 https://doi.org/10.1016/j.icheatmasstransfer.2021.105202.

Xiong, T., Zheng, L., Shah, K.W., 2020. Nano-enhanced phase change materials (NePCMs): a review of numerical simulations. Appl. Therm. Eng. 178, 115492 https://doi.org/10.1016/j.applthermaleng.2020.115492.

Yang, H., Yu, H.S., Chen, X., Zhuang, P.Z., 2023. Rigorous solution for drained analysis of spherical cavity expansion in soils of finite radial extent. Comput. Geotech. 160, 105516 https://doi.org/10.1016/j.compgeo.2023.105516.

Yao, P., Zhai, Y., Li, Z., Shen, X., Wang, H., 2021. Thermal performance analysis of multi-objective optimized microchannels with triangular cavity and rib based on field synergy principle. Case Stud. Therm. Eng. 25, 100963 https://doi.org/10.1016/j.csite.2021.100963.

Zadeh, S.M.H., Sabour, M., Sazgara, S., Ghalambaz, M., 2020. Free convection flow and heat transfer of nanofluids in a cavity with conjugate solid triangular blocks: employing Buongiorno's mathematical model. Phys. A: Stat. Mech. Appl. 538, 122826 https://doi.org/10.1016/j.physa.2019.122826.

Update

Energy Reports
Volume 11, Issue , June 2024, Page 249

DOI: https://doi.org/10.1016/j.egyr.2023.11.055

Energy Reports 11 (2024) 249–249

Contents lists available at ScienceDirect

Energy Reports

journal homepage: www.elsevier.com/locate/egyr

Corrigendum

Corrigendum to "Analysis of heat transfer in various cavity geometries with and without nano-enhanced phase change material: A review" [Energy Rep. 10 (2023) 3757–3779]

Farhan Lafta Rashid [a], Hayder I. Mohammed [b], Anmar Dulaimi [c,d,*], Mudhar A. Al-Obaidi [e,f], Pouyan Talebizadehsardari [g], Shabbir Ahmad [h], Arman Ameen [i]

[a] Petroleum Engineering Department, College of Engineering, University of Kerbala, Karbala 56001, Iraq
[b] Department of Physics, College of Education, University of Garmian, Kalar 46021, Kurdistan, Iraq
[c] College of Engineering, University of Warith Al-Anbiyaa, Karbala 56001, Iraq
[d] School of Civil Engineering and Built Environment, Liverpool John Moores University, Liverpool L3 2ET, UK
[e] Technical Institute of Baquba, Middle Technical University, Baghdad 10074, Iraq
[f] Technical Instructor Training Institute, Middle Technical University, Baghdad 10074, Iraq
[g] Power Electronics, Machines and Control (PEMC) Research Group, University of Nottingham, Nottingham, UK
[h] Department of Basic Sciences and Humanities, Muhammad Nawaz Sharif University of Engineering and Technology, Multan 60000, Pakistan
[i] Department of Building Engineering, Energy Systems and Sustainability Science, University of Gävle, 801 76 Gävle, Sweden

The authors regret that the affiliation of the author Pouyan Talebizadehsardari was wrongly written and should be changed to Power Electronics, Machines and Control (PEMC) Research Group, University of Nottingham, Nottingham, UK

So please modify the affiliation for the author Pouyan Talebizadehsardari as following:

Farhan Lafta Rashid[a], Hayder I Mohammed[b], Anmar Dulaimi[c d], Mudhar A. Al-Obaidi[e f], Pouyan Talebizadehsardari [g], Shabbir Ahmad [h], Arman Ameen[i]

[a] Petroleum Engineering Department, College of Engineering, University of Kerbala, Karbala 56001, Iraq

[b] Department of Physics, College of Education, University of Garmian, Kalar 46021, Kurdistan, Iraq

[c] College of Engineering, University of Warith Al-Anbiyaa, Karbala 56001, Iraq

[d] School of Civil Engineering and Built Environment, Liverpool John Moores University, Liverpool L3 2ET, UK

[e] Technical Institute of Baquba, Middle Technical University, Baghdad 10074, Iraq

[f] Technical Instructor Training Institute, Middle Technical University, Baghdad 10074, Iraq

[g] Power Electronics, Machines and Control (PEMC) Research Group, University of Nottingham, Nottingham, UK

[h] Department of Basic Sciences and Humanities, Muhammad Nawaz Sharif University of Engineering and Technology, Multan 60000, Pakistan

[i] Department of Building Engineering, Energy Systems and Sustainability Science, University of Gävle, 801 76 Gävle, Sweden

Thank you for your time and we are sorry for this inconvenience.

The authors would like to apologise for any inconvenience caused.

DOI of original article: https://doi.org/10.1016/j.egyr.2023.10.036.
* Corresponding author at: College of Engineering, University of Warith Al-Anbiyaa, Karbala 56001, Iraq.
E-mail address: a.f.dulaimi@ljmu.ac.uk (A. Dulaimi).

https://doi.org/10.1016/j.egyr.2023.11.055

Available online 6 December 2023